Z. Phys. C – Particles and Fields 21, 167–188 (1983)

Zeitschrift für Physik C Particles and Fields

Calculation of the Glueball Mass Spectrum of $SU(2)$ and $SU(3)$ Non-Abelian Lattice Gauge Theories II: $SU(3)$

K. Ishikawa

City College, CUNY, New York, NY 10033, USA

A. Sato

LICEPP, University of Tokyo, Tokyo, Japan

G. Schierholz

II. Institut für Theoretische Physik der Universität Hamburg, D-2000 Hamburg 50, Federal Republic of Germany

M. Teper

L.A.P.P., F-74000 Annecy-le-Vieux, France

Received August 19, 1983

Abstract. We calculate the glueball mass spectrum in the $SU(3)$ lattice regularized gauge theory. We find four *light* glueballs: the 0^{++}, 2^{++}, 0^{-+} and, most interestingly from the experimental point of view, the oddball 1^{-+}. We calculate the 0^{++} and 2^{++} masses over a range of β values and find that *both* states conform to continuum renormalization group behaviour to a very significant degree. The question of metastable states and temperature is addressed in detail. Finally we discuss and resolve contrary claims in the recent literature.

I. Introduction

Quantum chromodynamics (QCD) implies that gluon degrees of freedom should play as important a role as quark degrees of freedom in the hadron spectrum. The simple interpretation of the prominent low-lying hadron as (anti-)quark bound states implies the presence of a further sector of the hadron spectrum composed primarily of gluon degrees of freedom: the glueballs [1]. The absence of any firm experimental glueball candidates encourages a theoretical calculation of the glueball spectrum.

In this paper we perform a variational calculation of the glueball masses in the $SU(3)$ lattice-regularized [2] gauge theory, using Monte Carlo techniques [3, 4] for evaluating the Euclidean Feynman path integral. In the companion paper [5] we have presented the calculation of the $SU(2)$ glueball spectrum. We refer the reader to that paper for a more detailed discussion of the techniques we use.

Some of our results, in both the $SU(2)$ [6] and the $SU(3)$ [7] cases, have already appeared in earlier publications. In addition, there has been a separate attempt to calculate the glueball spectrum by Berg and Billoire [8], and a further calculation of the 0^{++} mass has been performed by Michael and Teasdale [9]. We shall compare all these calculations later in the paper.

Clearly the most important glueball states are those with light masses. We find four such states: the 0^{++}, 2^{++}, 0^{-+} and 1^{-+}. To check whether our results do indeed characterize the continuum limit, we repeat the 0^{++} and 2^{++} calculations at several values of the bare coupling and search for the continuum renormalization group behaviour of the two masses. Our results *do* show such a behaviour to a significant degree. The observation of this scaling for the 2^{++} state, and the lightness of the 1^{-+} state, contradict claims to the contrary by the authors of

[8] (they do not calculate the 0^{-+} mass). Later in this paper we shall examine these discrepancies in detail and show why they occur: the essential reason is that for all states except the 0^{++} what the authors of [8] really calculate are mass *upper bounds*. Hence their conclusion that only their 0^{++} state is relevant is not disturbing.

Apart from checking for the desired scaling behaviour of the 0^{++} and 2^{++} masses, we shall go in some detail into the question of metastable states and temperature on our spatially small lattices. Other checks on our calculations have been performed in the $SU(2)$ case ($SU(2)$ calculations are a factor of $O(10)$ faster than $SU(3)$ ones) and we encourage the reader to find them in [5]. We have also compared the efficiencies of different updating procedures and random number generators. This is discussed in the Appendix.

Calculating the Mass Spectrum [5]

Let $\phi(t)$ be a colour singlet, zero-momentum operator, localized at time t with some J^{PC} quantum numbers. Then

$$\frac{\langle\phi(t)\,\phi(0)\rangle}{\langle\phi(0)\,\phi(0)\rangle}=\frac{\langle\phi(0)\,e^{-Ht}\,\phi(0)\rangle}{\langle\phi(0)\,\phi(0)\rangle}$$
$$=\sum_{\substack{n=0\\ m_n\leqq m_{n+1}}}^{\infty} e^{-m_n t}\frac{|\langle\Omega|\,\phi\,|n\rangle|^2}{\sum_{n=0}^{\infty}|\langle\Omega|\,\phi\,|n\rangle|^2}$$
$$\leqq e^{-m_0 t}, \tag{1}$$

and clearly

$$m(J^{PC})\equiv m_0=\lim_{t\to\infty}\frac{1}{t}\ln\frac{\langle\phi(0)\,\phi(0)\rangle}{\langle\phi(t)\,\phi(0)\rangle}, \tag{2}$$

where $m(J^{PC})$ is the lowest glueball mass in the J^{PC} channel (we always impose $\langle\phi\rangle=0$).

Suppose, to the required precision of the calculation,

$$\langle\phi(t)\,\phi(0)\rangle\underset{t\geqq t_c}{\sim}e^{-mt}, \tag{3}$$

then

$$m\approx\frac{1}{t'-t}\ln\frac{\langle\phi(t)\,\phi(0)\rangle}{\langle\phi(t')\,\phi(0)\rangle}\bigg|_{t,t'\geqq t_c}. \tag{4}$$

In general (4) will be valid for smaller t, t' than (2). This is important since we can only use $\langle\phi(t)\,\phi(0)\rangle$ for values of t not so large that the signal is lost in statistical noise.

It is clear that t_c will be smaller the larger is the projection of ϕ onto the glueball wave-functional. This suggests using a variational type of calculation.

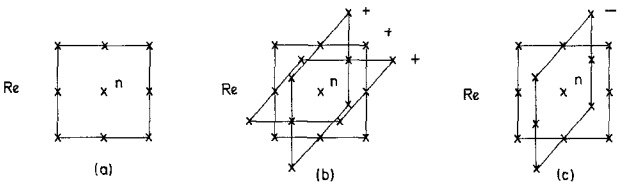

Fig. 1. a A 2×2 loop of link matrices, **b** a 0^{++} combination of 2×2 loops, **c** a 2^{++} combination of 2×2 loops

Let $t'>t$ be two times at which we can obtain accurate data and for which we can hope to find a wavefunction such that $\langle\phi(t \text{ and } t')\,\phi(0)\rangle$ is dominated by the lowest-lying glueball contribution. We choose some set of trial wavefunctions $\{\phi\}$ and find the $\phi_{\max}\in\{\phi\}$ such that

$$\frac{\langle\phi_{\max}(t)\,\phi_{\max}(0)\rangle}{\langle\phi_{\max}(0)\,\phi_{\max}(0)\rangle}=\max_{\{\phi\}}\left[\frac{\langle\phi(t)\,\phi(0)\rangle}{\langle\phi(0)\,\phi(0)\rangle}\right]. \tag{5}$$

Then our best estimate for m will be

$$m=\frac{1}{t'-t}\ln\frac{\langle\phi_{\max}(t)\,\phi_{\max}(0)\rangle}{\langle\phi_{\max}(t')\,\phi_{\max}(0)\rangle}. \tag{6}$$

The above is only one possible way to incorporate a variational improvement into the calculation: the best way will be determined by the pattern of statistical errors in the particular problem - see [5] for more details.

The trace of a closed loop of links is a colour singlet. If we sum all spatial translations of our initial loop we get a zero-momentum operator. By forming a suitable combination of various rotations of our initial loop we can isolate operators of differing lowest spin J. The real part of the trace has $C=+$, the imaginary part has $C=-$. By choosing a combination of loops that is invariant, or flips sign, under spatial inversion, we form operators of parity $+$ or $-$.

As an example take as the basic loop the real part of the trace of the 2×2 plaquette shown in Fig. 1a. In Fig. 1b we show the linear combination that has 0^{++} as its lowest J^{PC} quantum numbers. In Fig. 1c we show the 2^{++} linear combination.

For later convenience it is useful to introduce the notation

$$\Gamma_t\equiv\langle\phi(t)\,\phi(0)\rangle \tag{7}$$

for correlation functions.

II. The $SU(3)$ Calculation

The degrees of freedom of our lattice system are the 3×3 unitary matrices $U_\mu(n)$, where μ is the direction

of the link, out of the site n, on which the matrix resides. The partition function is

$$Z=\int \prod_{n,\mu} [dU_\mu(n)]\, e^{-S(U)}, \tag{8}$$

where the measure is the Haar invariant measure over the group. For the action S we shall use the Wilson action [2]

$$S(U)=\beta \sum_n (1-\tfrac{1}{3}\,\mathrm{Re}\,\mathrm{Tr}\,\square), \qquad \beta=\frac{6}{g^2}, \tag{9}$$

where $\mathrm{Tr}\,\square$ means taking the trace of the matrix obtained by multiplying together the 4 matrices on the links forming the plaquette. This action reproduces the usual continuum Euclidean action as the lattice spacing, a, goes to zero, and, when used with periodic boundary conditions (as we shall do), will ensure good positivity properties [10] even at finite lattice spacing.

For the Wilson action the relationship between the lattice spacing and β will be given by the usual two loop formula, once a is small enough:

$$a=\frac{83.5}{\Lambda_{\mathrm{mom}}} e^{-\frac{4\pi^2}{33}\beta} \left(\frac{8\pi^2}{33}\beta\right)^{\frac{51}{121}}. \tag{10}$$

We have replaced in (10) $\Lambda_{\mathrm{lattice}}$ with the more familiar Λ_{mom} [11]. We shall assume that for $\beta \geqq 5.5$ (10) is reliable. This is on the basis of previous work by other authors, in particular on measurements of the string tension [12].

In the Monte Carlo part of the calculation we generate the gauge field configurations using the heat bath routine of Pietarinen [12].

The Lattice Spacing in GeV^{-1} Units

The result of any mass calculation will, for dimensional reasons, take the form

$$ma = \text{some calculated number}. \tag{11}$$

To obtain m in physical GeV units we must know a in GeV^{-1} units. In principle we could use (10) with Λ_{mom} taken from deep inelastic experiments. However, such values of Λ_{mom} are notoriously ill-determined. The standard alternative procedure is to measure the string tension, $\sqrt{K}$, using ratios of Wilson loops [3, 12], and to equate it to the phenomenological value

$$\sqrt{K}=\left(\frac{1}{2\pi\alpha'}\right)^{\frac{1}{2}} \approx 400\,\mathrm{MeV}. \tag{12}$$

The recent high statistics study of Creutz and Moriarty [12] gives

$$\Lambda_{\mathrm{mom}}=(0.5\pm 0.1)\sqrt{K}. \tag{13}$$

Our own measurement [7] at a single value of β, $\beta=5.7$, gives

$$\Lambda_{\mathrm{mom}}=(0.48\pm 0.05)\sqrt{K}. \tag{14}$$

We infer from (13) and (14) the value

$$\Lambda_{\mathrm{mom}}=0.5\sqrt{K}=200\,\mathrm{MeV} \tag{15}$$

with an error of about $\pm(10\,\%$ to $20\,\%)$.

The relationship (12) is derived using an ideal string picture for the higher angular momentum states along a Regge trajectory. The fact that, unlike the real world, our lattice contains no fermion loops is probably not very important in this context: small fermion loops simply lead to a different β function, while larger loops have the primary role of giving the Regge trajectory an imaginary part and the hadrons a finite decay width, which, experimentally, is not large.

An alternative way of obtaining Λ_{mom} is through a calculation of the nonperturbative gluon condensate parameter, $\left\langle \frac{\alpha_s}{\pi} F^a_{\mu\nu} F^a_{\mu\nu} \right\rangle$, which plays an important role in the QCD sum rule calculations [13]. A recent lattice calculation [14] gives a value

$$\left\langle \frac{\alpha_s}{\pi} F^a_{\mu\nu} F^a_{\mu\nu} \right\rangle \approx (260\text{–}300\,\mathrm{MeV})^4 \tag{16}$$

if we use (15), to be compared to recent QCD sum rule estimates [15] of $(\approx 350\,\mathrm{MeV})^4$. This confirms that the value $\Lambda_{\mathrm{mom}}=200\,\mathrm{MeV}$ is in the right ball park.

In the remainder of the paper we shall use (15) to set the scale of the lattice in GeV units. The error of, presumably, $\pm O(10\,\%)$ will be suppressed but should not be forgotten.

Choosing the Lattice and Lattice Parameters

Let a_s, a_t be the spatial and temporal lattice spacings of our $L_s^3 \cdot L_t$ lattice (whenever we simply write a we mean $a \equiv a_s = a_t$) and let D_G be the diameter of the glueball. In order that the lattice should be neither too coarse, nor too small, nor too hot we require that

$$\min\left(\frac{L_t a_t}{2}, \frac{L_s a_s}{2}\right) > D_G > \max(a_t, a_s) \tag{17}$$

and

$$T(=\text{temperature})=\frac{1}{L_t a_t}\ll 200\,\text{MeV}. \tag{18}$$

To estimate D_G we calculate Γ_a/Γ_0 for 0^{++} wavefunctions composed of 1×1, 1×2 and 2×2 plaquettes on a $4^3\cdot8$ lattice at various values of β. In Fig. 2 we plot the results (how the common factor, at each β, of e^{ma} is obtained will become clearer later). We infer [16] that

$$D_G\approx(1.5\text{–}2.0)\,a(\beta=5.7). \tag{19}$$

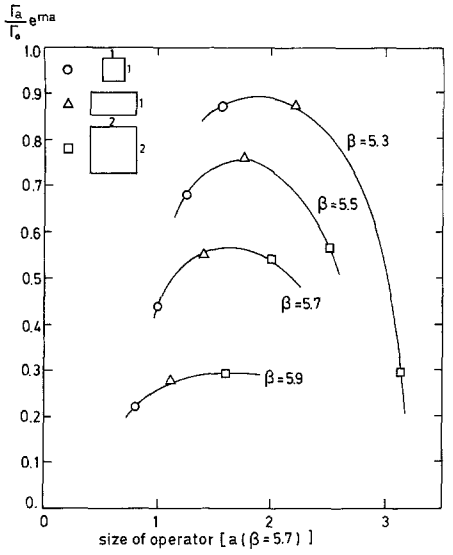

Fig. 2. Γ_a/Γ_0 for various operators versus the size of the operators in units of the $\beta=5.7$ lattice spacing

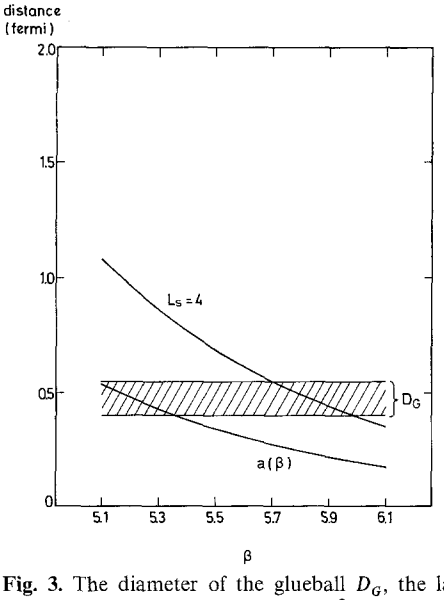

Fig. 3. The diameter of the glueball D_G, the lattice spacing and half the lattice spatial extent (for a $4^3\cdot L_t$ lattice) versus β

In Fig. 3 we plot the lattice spacing a, half the spatial lattice extent $\frac{1}{2}L_s a$ and the glueball size, D_G, for a lattice with $L_s=4$. The vertical scale is in fermi using (10) and (15). It is apparent that a lattice with $L_s=4$ will satisfy (17) in the range $5.3\lesssim\beta\lesssim5.9$ to a large degree. If we now pick $L_t=8$, then the temperature ranges from ≈60 to ≈120 MeV in this range of β values, so (18) is also satisfied.

In addition, we note that the string tension crossover region [12] seems to occur in the range $5.0\lesssim\beta\lesssim5.4$, with the correct continuum renormalization group behaviour setting in immediately afterwards.

All the above suggest that it is not naive to attempt to do continuum glueball physics with a $4^3\cdot8$ lattice for $5.4\lesssim\beta\lesssim5.9$.

The reason [5] we wish to minimise the spatial extent of the lattice (and $L_s=4$ is the smallest value of L_s that can possibly satisfy (17)!) is that a given gauge field configuration will give us only L_t measurements of a $\mathbf{p}=0$ correlation function: hence for a given error-to-signal ratio our computing time increases as L_s^3.

The strategy of our calculation will therefore be as follows. We shall first perform high statistics calculations for the 0^{++} and 2^{++} masses as deep in the continuum as possible. (That this is a practical task we infer from our $SU(2)$ studies [5].) We shall use a $4^3\cdot8$ lattice with equal spatial and temporal lattice spacings and shall perform calculations at $\beta=5.1$, 5.3, 5.5, 5.7 and 5.9. This will give us an extended lever arm for testing the renormalization group dependence of the masses, although one has to bear in mind that $\beta=5.1$ and 5.3 are in the string tension crossover region. From our ($\mathbf{p}=0$) $SU(2)$ work we expect to have a low-lying 0^{-+} state. The calculation of the relevant correlation functions is very lengthy, so we originally modified our usual procedure by using local rather than translation invariant operators [5]. This means our wave-functional will possess a non-zero momentum, which can be estimated using the 2^{++} mass. The advantage is of course an increase in statistics: one obtains $O(L_s^3)\cdot L_t$ measurements per configuration instead of L_t. The price one pays is an extra systematic error that derives from subtracting the momentum smearing. This early calculation of the 0^{-+} correlation function will later on be supplemented by a calculation of the (true) zero-momentum correlation function on an asymmetric lattice giving identical results.

The difficulty with extracting the masses of heavier glueballs is that the e^{-mt} decay of the correlation functions is very steep for larger m, and the ratio Γ_{2a}/Γ_a that we would like to use for estimating the mass gets quickly lost in statistical noise. To

overcome this difficulty we turn to a $4^3 \cdot 16$ lattice with

$$a_t < a_s. \tag{20}$$

To implement this we alter the Wilson action with the introduction of spatial and temporal inverse couplings

$$\beta \sum_{\text{all}} \mathrm{Re\,Tr}\,\square \to \beta_s \sum_{\text{spatial}} \mathrm{Re\,Tr}\,\square + \beta_t \sum_{\text{temporal}} \mathrm{Re\,Tr}\,\square, \tag{21}$$

so that

$$\beta_s/\beta_t = (a_t/a_s)^2, \tag{22}$$

ignoring perturbative corrections. The perturbative corrections alter (22) (and (10)) in a known [17] (to lowest order) way. Aiming for

$$a_s \approx a(\beta = 5.8), \quad a_t \approx 0.5\, a_s \tag{23}$$

we use

$$\beta_s = 3.3, \quad \beta_t = 10.68. \tag{24}$$

On this lattice we calculate with *zero-momentum operators* the 0^{++}, 2^{++}, and 0^{-+} glueball masses. We set the scale using the 0^{++} mass (since higher order corrections can break the connection between (23) and (24)). To reduce the statistical errors we repeat the calculation with local operators: this also gives us mass estimates for the heavier 0^{--}, 2^{--} and 1^{+-} glueballs. These glueballs are so heavy that the effects of momentum smearing are small and introduce no appreciable systematic errors into the final mass estimates.

Specific Heat

It was originally observed by Lautrup and Nauenberg [18] that the $SU(2)$ lattice specific heat

$$C = \beta^2 \frac{\partial}{\partial \beta} \langle \tfrac{1}{2} \mathrm{Tr}\,\square \rangle \tag{25}$$

peaks strongly near and just after the string tension cross-over region suggesting a nearby singularity in the complex, or mixed-action, β plane. Subsequent studies [19] found a similar structure for $SU(N)$, $N = 3, 4, 5, 6$, lattice gauge theories. (Indeed for $N \geqq 4$ the singularity appears to [19] cross the real axis, so that the theory develops a first order phase transition.) In Fig. 4a we plot our measurements of C/β^2 for the $4^3 \cdot 8$ lattice with $a_s = a_t$. In Fig. 4b we plot C/β^2 for the $4^3 \cdot 16$ lattice with $\beta_s/\beta_t = 3.3/10.68$. The

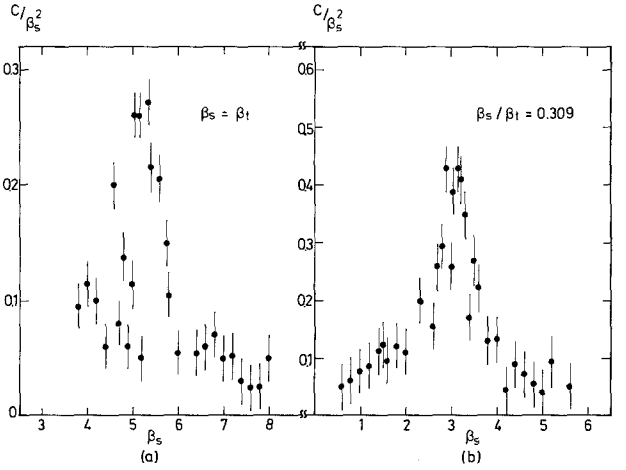

Fig. 4a and b. The specific heat divided by β_s^2: **a** for the $4^3 \cdot 8$ lattice with $\beta_s = \beta_t$, **b** for the $4^3 \cdot 16$ lattice with $\beta_s/\beta_t = 0.309$

peaks are apparent and it is also apparent that many of our measurements are taken quite high up the sides of this peak. The extent to which the peak reflects the onset of continuum physics, and the extent to which it represents effects that are merely a lattice artifact is, however, still obscure.

Glueball Masses on the $4^3 \cdot 8$ Lattice

At each β value we generate our gauge field configurations in several independent sequences. Each sequence begins with an independent initial configuration, obtained by upgrading the lattice at a random β value, and is brought to equilibrium at the desired β value with a generous $\simeq 300$ configurations. This procedure makes statistical error estimates particularly painless and minimises any danger of very long range correlations systematically biasing our results. The configurations are generated by a systematic upgrading of the links of the lattice using Pietarinen's $SU(3)$ heat bath routine [12].

At $\beta = 5.9$ we generate 25,000 configurations, at $\beta = 5.7$ about 27,000, at $\beta = 5.5$ about 11,000, at $\beta = 5.3$ about 19,000, and at $\beta = 5.1$ about 9,000.

(a) 0^{++} and 2^{++}. The 0^{++} and 2^{++} wave-functionals are constructed from the 1×1, 1×2 and 2×2 plaquettes in appropriate linear combinations as in Fig. 1. We adopt as generic labels for these operators ϕ_{11}, ϕ_{12} and ϕ_{22}, respectively. For spacelike plaquettes we project onto "magnetic" glueballs, 0_M^{++} and 2_M^{++}. The timelike 1×1 and 1×2 plaquettes (one step in time) generate us "electric" glueballs, 0_E^{++} and 2_E^{++}. (The electric states are less reliable in that their timelike extent is not infini-

Table 1. Ratios of correlation functions for 0_M^{++} on the $4^3 \cdot 8$ lattice

β	operator	Γ_a/Γ_0	Γ_{2a}/Γ_a	Γ_{3a}/Γ_{2a}
5.9	(1,1)	0.092±0.002	0.107±0.040	0.38±0.11
	(1,2)	0.116±0.002	0.154±0.010	0.28±0.04
	(2,2)	0.121±0.002	0.216±0.007	0.42±0.07
	max.	0.121±0.002	0.216±0.007	0.42±0.07
5.7	(1,1)	0.159±0.002	0.316±0.019	
	(1,2)	0.200±0.004	0.340±0.026	
	(2,2)	0.195±0.002	0.378±0.013	
	max.	0.214±0.003	0.361±0.018	
5.5	(1,1)	0.214±0.002	0.343±0.011	0.36±0.03
	(1,2)	0.241±0.002	0.332±0.006	0.38±0.02
	(2,2)	0.179±0.002	0.322±0.008	0.33±0.05
	max.	0.248±0.002	0.335±0.011	0.36±0.04
5.3	(1,1)	0.141±0.002	0.216±0.024	0.38±0.07
	(1,2)	0.146±0.002	0.213±0.011	0.46±0.04
	(2,2)	0.067±0.003	0.201±0.020	0.32±0.05
	max.	0.152±0.002	0.220±0.025	0.38±0.07
5.1	(1,1)	0.080±0.004	0.090±0.020	
	(1,2)	0.075±0.005	0.117±0.023	
	(2,2)	0.023±0.004	0.272±0.064	
	max.	0.083±0.004	0.105±0.020	

tesimal relative to the distances over which the correlation functions are measured.)

In Table 1 we present our results for ratios of correlation functions for 0_M^{++}. In addition to giving values for each of the three operators, we also find the linear combination $\phi_{\max}$ which maximises Γ_a/Γ_0 and present the corresponding values of Γ_{2a}/Γ_a and Γ_{3a}/Γ_{2a} (when significant; in our first run at $\beta=5.7$ Γ_{3a}/Γ_{2a} was not calculated). The linear combinations are

$$\begin{aligned}
&\phi_{\max}(\beta=5.9)\approx\phi_{22},\\
&\phi_{\max}(\beta=5.7)=0.23\,\phi_{11}+0.45\,\phi_{12}+0.87\,\phi_{22},\\
&\phi_{\max}(\beta=5.5)=0.75\,\phi_{11}+0.43\,\phi_{12}+0.50\,\phi_{22},\\
&\phi_{\max}(\beta=5.3)=0.85\,\phi_{11}+0.49\,\phi_{12}+0.19\,\phi_{22},\\
&\phi_{\max}(\beta=5.1)\approx 0.85\,\phi_{11}+0.49\,\phi_{12}+0.19\,\phi_{22}. \qquad (26)
\end{aligned}$$

Our procedure for obtaining mass estimates is motivated by the following observations. Consider Γ_a/Γ_0. We write it as

$$\Gamma_a/\Gamma_0=\alpha e^{-ma}+(1-\alpha)\,e^{-Ma}, \qquad (27)$$

where m is the desired glueball mass and M is the average mass of the excited states. If α is not too small, and a is not small on the scale of M, we have

$$\Gamma_a/\Gamma_0\approx\alpha e^{-ma}. \qquad (28)$$

Given that the glueball size is

$$D_G\approx(1.5\text{-}2.0)\,a(\beta=5.7)\approx a(\beta=5.1), \qquad (29)$$

the 1×1 plaquette should be a good wavefunction, i.e. $\alpha\simeq1$ at $\beta=5.1$ (this we will substantiate later on), simply because it is the smallest loop one can construct. Moreover, at these values of β $a(\beta)$ is quite large, so to a reasonable approximation we can (in principle) expect

$$ma\approx\ln\alpha+\ln\frac{\Gamma_0}{\Gamma_a}\approx\ln\frac{\Gamma_0}{\Gamma_a}. \qquad (30)$$

This is even more so for the 2_M^{++}, which is appreciably heavier and results in an appreciably larger Γ_0/Γ_a.

As β increases, α decreases and any estimate of it becomes increasingly unreliable. If α is still quite large, say $\alpha\approx0.5$, then Γ_a will still be dominated by the lowest glueball contribution, and a reliable estimate of ma can be obtained from the (harder to obtain) ratio Γ_{2a}/Γ_a:

$$ma=\ln\frac{\Gamma_a}{\Gamma_{2a}}. \qquad (31)$$

The pattern of values in Table 1 indicates this to be a good procedure for $\beta=5.1$, 5.3, 5.5 and 5.7.

We expect, however, that as β increases further, and the glueball size becomes more than 2 lattice units across, the planar character of simple loops such as ours will become manifest, and the projection onto the lowest glueball state will collapse dramatically. This begins to happen at $\beta=5.9$. Now both terms in (27) are important, so that Γ_{2a}/Γ_a is no longer a reliable measure of e^{-ma} even if Γ_{2a} is still dominated by e^{-ma} (as, for a while yet, it will):

$$\frac{\Gamma_{2a}}{\Gamma_a}\approx\frac{\alpha e^{-2ma}}{\alpha e^{-ma}+(1-\alpha)\,e^{-Ma}}\not\approx e^{-ma}. \qquad (32)$$

This effect is compounded by the decrease of the exponents ($a(\beta)$ decreases as β increases). At this stage we have to use (the even harder to obtain) Γ_{3a}/Γ_{2a} for our mass estimate:

$$ma=\ln\frac{\Gamma_{2a}}{\Gamma_{3a}}. \qquad (33)$$

And so on.

Thus motivated we obtain our 0_M^{++} masses as follows. At $\beta=5.9$ we use (33) on our maximised wavefunction. At $\beta=5.7$, 5.5, 5.3 and 5.1 we use (31) on our maximised wavefunction. (We have also found a signal for Γ_{3a}/Γ_{2a} at $\beta=5.5$ and 5.3 as shown in Table 1. Within errors the values obtained for Γ_{3a}/Γ_{2a} are consistent with those for Γ_{2a}/Γ_a.)

We plot our measured values of α at $\beta=5.1$, 5.3, 5.5, 5.7 and 5.9 in Fig. 5 taking

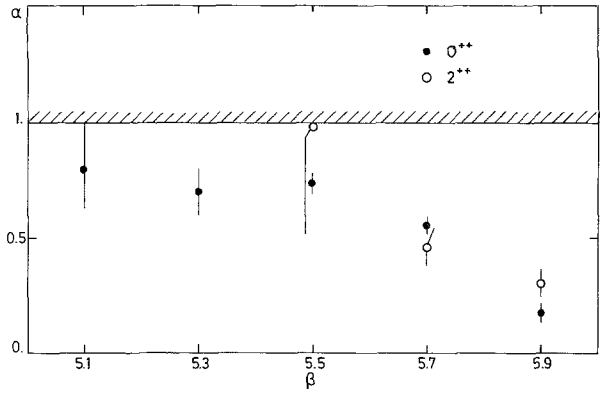

Fig. 5. The projection (probability) of the maximal wavefunction on the lowest 0^{++} and 2^{++} glueball states as a function of β

$$\alpha(\beta=5.9)=\left(\frac{\Gamma_{2a}}{\Gamma_0}\right)\left(\frac{\Gamma_{3a}}{\Gamma_{2a}}\right)^{-2}\Bigg|_{\beta=5.9} \tag{34}$$

and

$$\alpha(\beta)=\left(\frac{\Gamma_a}{\Gamma_0}\right)\left(\frac{\Gamma_{2a}}{\Gamma_a}\right)^{-1}\Bigg|_{\beta} \tag{35}$$

otherwise. The trend is clear (and as we have anticipated): α increases towards 1 as β decreases. This demonstrates that indeed our wavefunction becomes sort of ideal at smaller β.

In Table 4 we present our estimates of e^{-ma} and the mass m in GeV units (using (10) and (15)) for the 0_M^{++} glueball. We also present the corresponding values for the electric glueball 0_E^{++} in Tables 3 and 4.

We now repeat this procedure for the magnetic and electric 2^{++} glueballs. The values of the correlation functions for 2_M^{++} are tabulated in Table 2. It is clear that the 2_M^{++} is appreciably heavier than the 0_M^{++}. For this reason it is sufficient to use Γ_{2a}/Γ_a for our mass estimate at $\beta=5.9$. For the same reason we obtain no significant signal for Γ_{2a}/Γ_a at $\beta=5.3$ and 5.1 and large errors at $\beta=5.5$, so we shall (have to) take the largest Γ_a/Γ_0 there:

$$ma=\ln\alpha+\ln\frac{\Gamma_0}{\Gamma_a}\Bigg|_{\min}. \tag{36}$$

We plot our measured values of α at $\beta=5.5$, 5.7 and 5.9 in Fig. 5. The trend is the same as for the 0_M^{++} glueball. So for $\beta\leqq 5.5$ we may expect $0.8\lesssim\alpha\lesssim 1$, which gives the mass estimate at $\beta=5.5$ (cf. Table 2):

Table 2. Ratios of correlation functions for 2_M^{++} on the $4^3\cdot 8$ lattice

β	operator	Γ_a/Γ_0	Γ_{2a}/Γ_a
5.9	(1,1)	0.026±0.002	−0.006±0.149
	(1,2)	0.039±0.001	0.154±0.094
	(2,2)	0.049±0.001	0.166±0.038
	max.	0.051±0.001	0.163±0.037
5.7	(1,1)	0.032±0.002	0.062±0.016
	(1,2)	0.047±0.003	0.053±0.004
	(2,2)	0.049±0.003	0.150±0.025
	max.	0.055±0.002	0.107±0.020
5.5	(1,1)	0.033±0.002	−0.043±0.100
	(1,2)	0.042±0.002	0.015±0.010
	(2,2)	0.029±0.002	0.168±0.010
	max.	0.044±0.002	0.034±0.050
5.3	(1,1)	0.032±0.002	
	(1,2)	0.031±0.002	
	(2,2)	0.013±0.003	
	max.	0.034±0.002	
5.1	(1,1)	0.024±0.002	
	(1,2)	0.026±0.002	
	(2,2)	0.008±0.002	
	max.	0.028±0.002	

Table 3. Ratios of correlation functions for 0_E^{++} and 2_E^{++} on the $4^3\cdot 8$ lattice

β	J^{PC}	operator	Γ_a/Γ_0	Γ_{2a}/Γ_a	Γ_{3a}/Γ_{2a}
5.9	0_E^{++}	(1,1)	0.067±0.003	0.167±0.024	0.310±0.187
		(1,2)	0.092±0.003	0.168±0.021	0.295±0.254
		max.	0.092±0.003	0.168±0.021	0.295±0.254
	2_E^{++}	(1,1)	0.012±0.001	−0.269±0.076	
		(1,2)	0.031±0.002	0.113±0.040	
		max.	0.031±0.002	0.113±0.040	
5.7	0_E^{++}	(1,1)	0.123±0.003	0.330±0.062	
		(1,2)	0.147±0.003	0.329±0.044	
		max.	0.150±0.003	0.330±0.047	
	2_E^{++}	(1,1)	0.011±0.003	0.205±0.153	
		(1,2)	0.024±0.001	0.214±0.041	
		max.	0.024±0.001	0.208±0.055	
5.5	0_E^{++}	(1,1)	0.154±0.004	0.319±0.012	
		(1,2)	0.155±0.004	0.332±0.014	
		max.	0.167±0.004	0.329±0.014	
	2_E^{++}	(1,1)	0.013±0.001	0.367±0.064	
		(1,2)	0.013±0.002	0.134±0.038	
		max.	0.015±0.001	0.201±0.050	
5.3	0_E^{++}	(1,1)	0.082±0.004	0.285±0.044	
		(1,2)	0.071±0.005	0.273±0.042	
		max.	0.085±0.004	0.281±0.044	
	2_E^{++}	(1,1)	0.002±0.001		
		(1,2)	0.003±0.001		
		max.	0.003±0.001		
5.1	0_E^{++}	(1,1)	0.036±0.002	0.141±0.063	
		(1,2)	0.026±0.002	0.306±0.055	
		max.	0.036±0.002	0.168±0.063	
	2_E^{++}	(1,1)	0.003±0.001		
		(1,2)	0.001±0.003		
		max.	0.003±0.001		

Table 4. 0^{++} and 2^{++} masses on the $4^3 \cdot 8$ lattice

β		0_M^{++}	0_E^{++}	2_M^{++}	2_E^{++}
5.9	e^{-ma}	0.42 ± 0.07		0.163 ± 0.037	$0.295^{+0.254}_{-0.148}$
	m (GeV)	$0.79^{+0.17}_{-0.14}$		$1.66^{+0.23}_{-0.19}$	$1.11^{+0.64}_{-0.56}$
5.7	e^{-ma}	0.361 ± 0.018	0.330 ± 0.047	0.107 ± 0.020	0.208 ± 0.055
	m (GeV)	0.74 ± 0.04	0.81 ± 0.10	$1.63^{+0.15}_{-0.13}$	$1.15^{+0.22}_{-0.18}$
5.5	e^{-ma}	0.335 ± 0.011	0.329 ± 0.014	$0.044^{+0.014}_{-0.002}$	0.201 ± 0.050
	m (GeV)	0.64 ± 0.02	$0.65^{+0.02}_{-0.03}$	$1.81^{+0.02}_{-0.15}$	$0.93^{+0.17}_{-0.13}$
5.3	e^{-ma}	0.220 ± 0.025	0.281 ± 0.044	$0.034^{+0.011}_{-0.002}$	$\geqq 0.003 \pm 0.001$
	m (GeV)	$0.70^{+0.06}_{-0.05}$	$0.59^{+0.08}_{-0.07}$	$1.57^{+0.03}_{-0.13}$	
5.1	e^{-ma}	0.105 ± 0.020	0.168 ± 0.063	$0.028^{+0.010}_{-0.002}$	$\geqq 0.003 \pm 0.001$
	m (GeV)	$0.84^{+0.08}_{-0.06}$	$0.67^{+0.17}_{-0.12}$	$1.33^{+0.03}_{-0.11}$	

$$e^{-ma} = \alpha^{-1} \left.\frac{\Gamma_a}{\Gamma_0}\right|_{\max}$$
$$= \alpha^{-1}(0.044 \pm 0.002)$$
$$\approx 0.044^{+0.014}_{-0.002} \tag{37}$$

and

$$ma = 3.12 \pm 0.04 + \ln \alpha$$
$$\approx 3.12 \pm^{0.04}_{0.26}, \tag{38}$$

and similarly at $\beta = 5.3$ and 5.1. Note that for α being even as low as 0.6 the error in (38) will only increase to about 15% due to the large lattice spacing and 2_M^{++} mass. This is to say that the pure variational calculation gives reasonable mass estimates here.

Our maximal 2_M^{++} wavefunctions are

$$\phi_{\max}(\beta = 5.9) = 0.15\,\phi_{11} + 0.15\,\phi_{12} + 0.98\,\phi_{22},$$
$$\phi_{\max}(\beta = 5.7) = 0.20\,\phi_{11} + 0.45\,\phi_{12} + 0.87\,\phi_{22},$$
$$\phi_{\max}(\beta = 5.5) = 0.43\,\phi_{11} + 0.75\,\phi_{12} + 0.50\,\phi_{22},$$
$$\phi_{\max}(\beta = 5.3) = 0.85\,\phi_{11} + 0.49\,\phi_{12} + 0.19\,\phi_{22},$$
$$\phi_{\max}(\beta = 5.1) \approx 0.85\,\phi_{11} + 0.49\,\phi_{12} + 0.19\,\phi_{22}. \tag{39}$$

Our final mass estimates appear in Table 4. The error on the $\beta = 5.5$ and 5.3 2_M^{++} masses are dominated by the error in the estimate of $\alpha(\beta)$. At $\beta = 5.1$ the statistical error dominates. The corresponding values of the correlation functions and the mass estimates for the electric glueball 2_E^{++} are presented in Tables 3 and 4.

Although our detailed procedure for extracting the masses is entirely plausible, the only real way to check if it is really correct would be to do a very high statistics study on a large L_t lattice and to check that indeed

$$\frac{\Gamma_{2a}}{\Gamma_a} \approx \frac{\Gamma_{3a}}{\Gamma_{2a}} \approx \frac{\Gamma_{4a}}{\Gamma_{3a}} \cdots . \tag{40}$$

This we do not do here for reasons of computer time. In the faster $SU(2)$ case, however, we have obtained [5] measurements of the correlation functions up to 12 lattice spacings on a $5^3 \cdot 40$ lattice with

$$a_t = 0.25\, a_s, \tag{41}$$

and the resulting fine-grained version of (40) confirms the validity of our equivalent mass estimate procedures in the equivalent range of couplings. A much more modest $SU(3)$ version of such a check will be described later on in this paper.

The electric glueball states are broadly compatible, within large errors, with the results for the magnetic states. From now on we shall ignore the electric states and drop the magnetic label.

(b) Renormalization Group Behaviour. The statement of renormalization group behaviour is simply that our calculated glueball mass, when expressed in terms of a fixed scale via the continuum renormalization group equation for $a(\beta)$, should *not* depend on the bare coupling, β.

Accordingly we plot in Fig. 6 the glueball mass versus the value of β at which it is calculated in the dimensionless product form of $ma(\beta=5.7)$. We obtain this value from the measured quantity $ma(\beta)$ by the use of the two loop formula, (10). We could equally well have plotted m in GeV units, as it appears in Table 4. The only difference would involve an overall rescaling of the vertical axis.

We see that for $\beta \geqq 5.3$ both the 0^{++} and 2^{++} masses are indeed independent of β within their error bars, except for may be a slight dip (enhancement) in the $0_M^{++}(2_M^{++})$ at $\beta=5.5$, i.e. at the peak in the specific heat. The relative constancy remains striking even if we consider the whole range, $\beta \geqq 5.1$.

Given the finite size of the error bars, what is the significance of this? To answer this question we need some standard for what might be a natural rate of variation of m with β if we were *not* in the continuum limit. Such a standard is provided by the 2-loop $a(\beta)$ itself as given by (10), since we have scaled our experimental results with this functional dependence. From $\beta=5.1$ to $\beta=5.9$, the 2-loop $a(\beta)$, as plotted in Fig. 6, varies by a factor of ≈ 2.5. The systematic variation of the 0^{++} data in this region is less than a factor of 1.3 and for the 2^{++} less than a factor of 1.4. We conclude that both the 0^{++} and 2^{++} states display a significant adherence to the desired continuum renormalization group behaviour – implying that our mass estimates do indeed accurately characterize the continuum glueball masses.

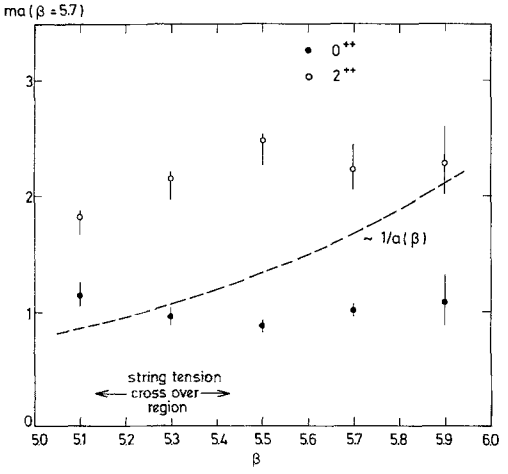

Fig. 6. 0^{++} and 2^{++} masses (in fixed units) versus β

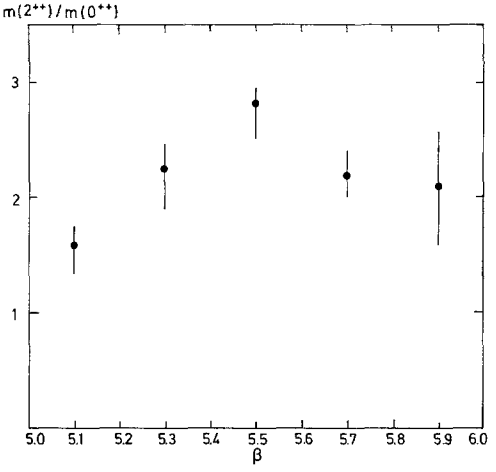

Fig. 7. The ratio of 2^{++} to 0^{++} glueball masses versus β

The deviation from continuum behaviour at $\beta=5.1$ (cf. Fig. 6) seems to involve a convergence of the 0^{++} and 2^{++} masses in the "cross-over region".

In Fig. 7 we plot the ratio of masses $m(2^{++})/m(0^{++})$ – note that in this ratio $a(\beta)$ cancels, so no 2-loop calculation is involved – to see this trend more explicitly. We remark that a decreasing $m(2^{++})/m(0^{++})$ ratio as β enters the strong coupling regime is indeed what one expects on the basis of strong coupling expansions [20]. However, the presence of a rapid variation of this ratio in the cross-over region, as suggested by Fig. 7, would be bad news for attempts to extrapolate the strong coupling expansions, in a smooth manner, through this region.

(c) 0^{-+}. The natural trial wavefunction for the 0^{-+} would be a lattice version of the $F\tilde{F}$ operator ("$\mathbf{E}\cdot\mathbf{B}$"), the topological charge density. We employ as our basic loop a variation on one of the standard [21] such versions:

$$\phi_{0^{-+}}(n)=\sum_{i,j,k=\pm 1}^{\pm 3}\tilde{\varepsilon}_{0ijk}\,\mathrm{Re\,Tr}[U_0(n)U_i(n+e_0)\cdot U_j(n+e_0+e_i)U_k(n+e_0+e_i+e_j)U_0^+(n+e_i+e_j+e_k)\cdot U_i^+(n+e_j+e_k)U_j^+(n+e_k)U_k^+(n)], \quad (42)$$

where the $\tilde{\varepsilon}_{\mu\nu\rho\sigma}$ tensor coincides with $\varepsilon_{\mu\nu\rho\sigma}$ for all indices positive and is extended to negative values by the definition $\tilde{\varepsilon}_{1\nu\rho\sigma}=-\tilde{\varepsilon}_{-1\nu\rho\sigma}$, following [21].

The numerical calculation of (42) is very slow. So, to obtain a mass estimate in a reasonable time, we first discarded our ideal procedure of using translation invariant, $\mathbf{p}=0$ operators (for the calculation of $\mathbf{p}=0$ 0^{-+} correlation functions see later on) and instead formed trial wavefunctionals out of clusters

of neighbouring (in all 3 spatial directions) loops. This increases the number of measurements by a factor of 8. The price we pay is that what we extract is an energy

$$(Ea)^2=(ma)^2+\overline{p^2} \tag{43}$$

involving an a priori unknown average momentum smearing. To estimate $\overline{p^2}$ we perform the same calculation for the 0^{++} and 2^{++} states, and substitute the already measured 0^{++} and 2^{++} masses in the corresponding relations (43). This gives us a consistent estimate

$$\overline{p^2}\approx 4/a^2. \tag{44}$$

Using this we find from Γ_a/Γ_0 the mass upper bound

$$m(0^{-+})\leqq(8.46\pm 0.20)\,\Lambda_{\mathrm{mom}} \tag{45}$$

and a mass estimate from Γ_{2a}/Γ_a of

$$m(0^{-+})=\left(7.2^{+1.6}_{-0.9}\right)\Lambda_{\mathrm{mom}} =1440^{+320}_{-180}\,\mathrm{MeV}. \tag{46}$$

Glueball Masses on the $4^3\cdot 16$ Lattice

We work with a lattice action as in (21), which allows us to vary the spatial and temporal lattice spacings, a_s and a_t, independently. We would like to work as deep in the continuum as our 4^3 spatial volume allows. So we choose couplings

$$\beta_s=3.3, \quad \beta_t=10.68, \tag{47}$$

which, according to the perturbative calculation [17] should correspond to

$$a_s\approx a(\beta=5.8), \quad a_t\approx 0.5\,a_s \tag{48}$$

in terms of our previous, hypercubic lattice spacing $a(\beta)$. This choice of a_t should be appropriate for high mass states. Since the perturbative, 1-loop calculation is not expected to be exact at these values of the coupling, our actual normalization of a_t will be performed by calculating ma_t for the 0^{++} glueball, and then inserting for m the value obtained in our calculation on the $4^3\cdot 8$ lattice. We will find that in fact

$$a_t=(0.737\pm 0.057)\,a(\beta=5.8), \tag{49}$$

showing significant $O(g^2)$ corrections to the perturbative 1-loop results [17]. This is in contrast to the $SU(2)$ case [5], where the perturbative estimate works very well. One must also check a_s. This we shall do later below and we confirm that

$$a_s\approx a(\beta=5.8). \tag{50}$$

Before we performed any measurements of the correlation functions we have generated $\simeq$4,000 configurations (upon which we measured the specific heat etc.). This ensures that our lattice is indeed in equilibrium. The correlation functions are measured upon a subsequent 6,000 gauge field configurations. Note that this is equivalent to 12,000 configurations on $4^3\cdot 8$. In addition we use a rather sophisticated upgrading procedure: the link to be upgraded next is chosen at random using a sequence of $\simeq 10^7$ *true* (physically generated) random numbers [22], and the actual upgrading is performed with a 60 bit multiplicative congruential random number generator [23]. This is in contrast to our previous calculations, where the links were chosen by sweeping systematically through the lattice, and where the generator used was often a 32 bit one. The reason for this extra effort is that we have some indication that the more massive states are sensitive to the procedure used. We refer the reader to the Appendix for a detailed discussion of all this.

(a) Glueball Masses. The basic loops we use for our operators are shown in Fig. 8. They will be referred to in the following by their length, which varies from 4 to 12 links. In addition, for the 0^{-+} state we use the $F\tilde{F}$ operator as in (42).

We form 0^{++}, 2^{++}, 0^{-+}, 1^{-+}, 0^{--}, 2^{--} and 1^{+-} *zero-momentum* operators by suitable combinations of translations, rotations, spatial inverses and real/imaginary parts of these basic loops.

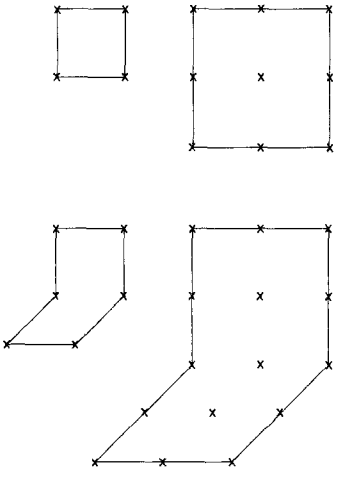

Fig. 8. Basic loops used to construct glueball operators on the $4^3\cdot 16$ lattice

The ratios of $\mathbf{p}=0$ correlation functions are shown in Table 5.

In Fig. 9 we plot the effective 0^{++} and 2^{++} mass as extracted from the ratios of correlation functions given in Table 5, i.e.

$$m_{\text{eff}}(n)\,a_t=\ln\left(\frac{\Gamma_{(n-1)}\,a_t}{\Gamma_n\,a_t}\right), \qquad n=1,2,3. \tag{51}$$

The 0^{++} $m_{\text{eff}}(n)$ shows very clearly that the lowest energy state already dominates the ratio $\Gamma_{3a_t}/\Gamma_{2a_t}$, i.e.

$$\Gamma_{2a_t}\approx\alpha e^{-2ma_t}, \qquad \Gamma_{3a_t}\approx\alpha e^{-3ma_t}. \tag{52}$$

Table 5. Ratios of correlation functions for 0^{++}, 2^{++}, 0^{-+}, 1^{-+}, 0^{--}, 2^{--} and 1^{+-} on the asymmetric $4^3\cdot 16$ lattice

J^{PC}	operator	Γ_{a_t}/Γ_0	$\Gamma_{2a_t}/\Gamma_{a_t}$	$\Gamma_{3a_t}/\Gamma_{2a_t}$
0^{++}	6	0.317 ± 0.01	0.414 ± 0.03	0.504 ± 0.06
	8	0.265 ± 0.007	0.382 ± 0.019	$0.51\ \pm0.03$
	12	0.239 ± 0.007	0.474 ± 0.034	$0.48\ \pm0.06$
2^{++}	4			$0.17\ \pm0.47$
	6	0.105 ± 0.003	0.138 ± 0.024	$0.35\ \pm0.17$
	8	0.130 ± 0.002	$0.23\ \pm0.02$	$0.19\ \pm0.20$
	12	0.050 ± 0.003	0.166 ± 0.048	$0.57\ \pm0.30$
0^{-+}	$F\tilde{F}$	-0.054 ± 0.003	$0.28\ \pm0.08$	
1^{-+}	6	0.080 ± 0.003	0.102 ± 0.022	
	12	0.040 ± 0.0014	0.201 ± 0.055	
0^{--}	6	0.021 ± 0.004	0.175 ± 0.14	
	12	0.013 ± 0.004	$-0.21\ \pm0.29$	
2^{--}	6	0.035 ± 0.002	$-0.02\ \pm0.05$	
	12	0.021 ± 0.002	$0.05\ \pm0.12$	
1^{+-}	6	0.044 ± 0.0025	$0.03\ \pm0.04$	
	8	0.050 ± 0.002	-0.005 ± 0.04	
	12	0.022 ± 0.002	$0.14\ \pm0.08$	

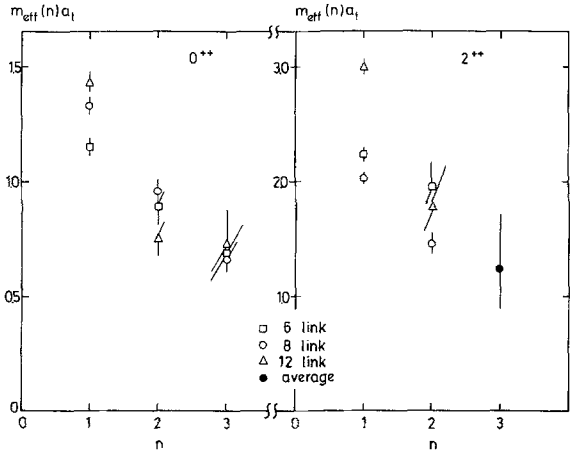

Fig. 9. The effective 0^{++} and 2^{++} masses (defined as local logarithmic derivatives of the correlation function) as functions of distance (in lattice spacings)

Comparing the value of ma_t obtained from Γ_{3a}/Γ_{2a} with our previous 0^{++} mass measurement on a $4^3\cdot 8$ lattice allows us to relate a_t to the hypercubic lattice spacing $a(\beta)$ as in (49).

To check the self-consistency of these comparisions we note that $a_t\approx 2/3\,a(\beta=5.7)$, so that

$$\frac{\Gamma_{2a(\beta=5.7)}}{\Gamma_{a(\beta=5.7)}}\approx\frac{\Gamma_{3a_t}}{\Gamma_{1.5a_t}}\approx\frac{\Gamma_{3a_t}}{(\Gamma_{a_t}\cdot\Gamma_{2a_t})^{\frac{1}{2}}}. \tag{53}$$

Since at $\beta=5.8$ the 8 link operator is of a different size and is a worse glueball wave-functional than at $\beta=5.7$, it is not the appropriate operator for a comparison. Instead we should use an operator here which has the same projection, $\alpha=0.59$, as the best operator at $\beta=5.7$. The 6 and 12 link operators have $\alpha=0.50$ and 0.44, respectively. For the average of these two operators we obtain

$$\frac{\Gamma_{3a_t}}{(\Gamma_{a_t}\cdot\Gamma_{2a_t})^{\frac{1}{2}}}=0.93\,e^{-1.5ma_t}=e^{-1.5\left(m+\frac{0.073}{1.5a_t}\right)a_t}, \tag{54}$$

indicating that our procedure on the $4^3\cdot 8$ lattice, at $\beta=5.7$, of extracting the 0^{++} mass from the ratio Γ_{2a}/Γ_a is accurate to $O(7\%)$, which is comparable to the statistical error. Since our best operator at $\beta=5.7$ is better than either of the two operators used in (54), the error should in fact be less than 7%.

We can estimate a_s by a similar argument. For the 2×2 plaquette the projection

$$\alpha(\beta_s=3.3,\beta_t=10.68)=\frac{\Gamma_{2a_t}}{\Gamma_0}e^{2ma_t}=0.39\pm0.025, \tag{55}$$

whereas for the same operator on the $4^3\cdot 8$ lattice we find

$$\alpha(\beta=5.7)=0.54\pm0.027,$$
$$\alpha(\beta=5.9)=0.16\pm0.035. \tag{56}$$

A straight-line interpolation on a graph of the kind in Fig. 5 gives us an estimate of

$$a_s=a(\beta=5.78\pm0.02), \tag{57}$$

being remarkably consistent with the perturbative expectation, (50). As a further check we have calculated parallel plaquette correlation functions along spacelike directions and compared with similar calculations on the $4^3\cdot 8$ lattice. Again we confirm (50), although less precisely.

Turning now to the 2^{++} glueball, the error on $\Gamma_{3a_t}/\Gamma_{2a_t}$ is too large to make it useful. However, we have seen (Fig. 9) that for the 0^{++} the maximal value of $\Gamma_{2a_t}/\Gamma_{a_t}$ will already provide an accurate mass estimate. For the heavier 2^{++} this should be even more the case. (That the 2^{++} *is* heavier can be

Table 6. 0^{++}, 2^{++}, 0^{-+}, 1^{-+}, 0^{--}, 2^{--} and 1^{+-} masses on the asymmetric $4^3 \cdot 16$ lattice

J^{PC}	ma_t	
	$\mathbf{p}=0$	$\delta\mathbf{p}$[b]
0^{++}	0.67 ± 0.04	
2^{++}	1.47 ± 0.09	
	$\left(1.24^{+0.5}_{-0.35}\right)$[a]	
0^{-+}	$1.27^{+0.33}_{-0.25}$	
1^{-+}	$1.60^{+0.32}_{-0.24}$	1.57 ± 0.17
0^{--}	$2.30^{+1.1}_{-0.7}$	2.61 ± 0.21
2^{--}	$2.8^{+0.6}_{-0.4}$	3.1 ± 0.2
1^{+-}	$2.8^{+0.2}_{-0.3}$	2.7 ± 0.12

[a] from $\Gamma_{3a_t}/\Gamma_{2a_t}$
[b] using $(Ea_t)^2 = (ma_t)^2 + (0.4 \pm 0.4)$

inferred from the values of $\Gamma_{3a_t}/\Gamma_{2a_t}$). Accordingly, in the spirit of the variational calculation, we ask which of the three wavefunctions maximises Γ_{2a_t}/Γ_0 and use the measured value of $\Gamma_{2a_t}/\Gamma_{a_t}$ for this wavefunction to extract the mass, i.e. we use the 8 link operator. This gives the value in Table 6.

For the 0^{-+} glueball we use a trial wave-functional based on the *zero-momentum* linear combination of the operator in (42). We extract the mass from the measured value of $\Gamma_{2a_t}/\Gamma_{a_t}$ (see Table 5). It is given in Table 6.

For the 1^{-+} both trial wave-functionals have equal values of Γ_{2a_t}/Γ_0; this introduces some ambiguity into how to implement the variational procedure. One way is to use the greater of the two values of $\Gamma_{2a_t}/\Gamma_{a_t}$, and we give the result in Table 6. We note that the alternative possibility of averaging the two values of $\Gamma_{2a_t}/\Gamma_{a_t}$ leads to a mass estimate that is consistent, within errors, with that in Table 6.

For the 0^{--}, 2^{--} and 1^{+-} states the errors are so large that the variational procedure is not useful. Instead we simply average all the values of $\Gamma_{2a_t}/\Gamma_{a_t}$ weighting with the inverse of the square of the statistical error, and using the Γ_{a_t}/Γ_0 for mass upper bounds where appropriate. The resulting mass estimates are given in Table 6.

We illustrate our procedure of the preceding paragraph with the 1^{+-} state. First we average $\Gamma_{2a_t}/\Gamma_{a_t}$ for the three values in Table 5:

$$\overline{\Gamma_{2a_t}/\Gamma_{a_t}} = 0.027 \pm 0.031, \tag{58}$$

where in the average we weight each term by the inverse of the error squared. Now we observe that the 8 link Γ_{a_t}/Γ_0 gives us the upper bound

$$e^{-ma_t} \geqq 0.048. \tag{59}$$

We impose (59) upon (58) as follows. We have a Gaussian random variable $x(\equiv \Gamma_{2a_t}/\Gamma_{a_t})$ with mean $\bar{x} = 0.027$ and $\sigma = 0.031$. Now we impose $x \geqq 0.048$. The resulting distribution is no longer normal. We define our new mean $\bar{y}$ and errors σ_+, σ_- by the requirement that

$$\begin{aligned}
&\text{probability } (0.048 \leqq x \leqq \bar{y}) = \text{probability } (x \geqq \bar{y}),\\
&\text{probability } (\bar{y} - \sigma_- \leqq x \leqq \bar{y})\\
&= \text{probability } (\bar{y} \leqq x \leqq \bar{y} + \sigma_+)\\
&= \tfrac{2}{3} \text{ probability } (x \geqq \bar{y}).
\end{aligned} \tag{60}$$

Using standard error function tables [24] we finally get the mass estimate

$$e^{-ma_t} = 0.063^{+0.018}_{-0.011}, \tag{61}$$

which translates into the mass value in Table 6. A similar procedure was followed for the 2^{--} state, while the 0^{--} was calculated by a straight average of the two $\Gamma_{2a_t}/\Gamma_{a_t}$ values.

Our final values for the various masses, Table 6, show that we have 3 relatively light excited glueball states, the 2^{++}, 0^{-+} and the oddball 1^{-+}, and three probably rather heavier states. The obvious intense interest of low-lying oddballs puts a strong premium on reducing the rather large statistical errors which, in this zero-momentum calculation, necessarily afflict our 1^{-+} and 0^{--} mass estimates. To reduce these errors in a reasonable time we must drop our restriction to wave-functionals that are translation invariant.

(b) Reducing Errors with Momentum-Smeared Wavefunctions. We repeat the calculation, for all the states except the 0^{-+}, using a spatially localized combination of our 6 link operator. We sum the basic loops about the 8 sites of the simple spatial cube. This gives us 8 measurements per configuration at each time versus 1 for $\mathbf{p}=0$ wavefunctions and correspondingly reduced errors.

Our results for ratios of correlation functions are given in Table 7. Since we are using localized wavefunctions what we extract is not the mass directly, but an energy:

$$(E(J^{PC})a_t)^2 = (m(J^{PC})a_t)^2 + \overline{p^2(J^{PC})}. \tag{62}$$

Since our wavefunctions all have the same geometric size, the momentum smearing $\overline{p^2(J^{PC})}$ should depend

Table 7. Ratios of correlation functions for 0^{++}, 2^{++}, 1^{-+}, 0^{--}, 2^{--} and 1^{+-} on the asymmetric $4^3 \cdot 16$ lattice, using momentum-smeared wavefunctions and 6-link operators only

J^{PC}	Γ_{a_t}/Γ_0	$\Gamma_{2a_t}/\Gamma_{a_t}$	$\Gamma_{3a_t}/\Gamma_{2a_t}$
0^{++}	0.165 ±0.001	0.227±0.003	0.244±0.017
2^{++}	0.114 ±0.001	0.162±0.003	0.226±0.02
1^{-+}	0.105 ±0.0007	0.146±0.003	0.184±0.02
0^{--}	0.0383±0.0007	0.068±0.0014	0.15 ±0.13
2^{--}	0.040 ±0.0005	0.044±0.007	
1^{+-}	0.043 ±0.0005	0.064±0.006	0.004±0.088

only on $m^2(J^{PC})$, and, in particular, it should be approximately the same for all masses satisfying

$$(ma_t)^2 \gg \overline{p^2}. \tag{63}$$

As expected, for the 0^{++} (63) is *not* true, so we cannot use it to obtain a useful $\overline{p^2}$. For the 2^{++}, however, we find (using $\Gamma_{3a_t}/\Gamma_{2a_t}$ from Table 7 and the $\mathbf{p}=0$ mass estimate in Table 6)

$$\overline{p^2} = 0.4 \pm 0.4 \ll (m(2^{++})a_t)^2 \approx 2. \tag{64}$$

Since it is already clear from our $\mathbf{p}=0$ mass estimates that none of the states being considered here is significantly lighter than the 2^{++}, (64) should provide an adequate estimate of $\overline{p^2}$ in all cases. Using (62), (64) and the $\Gamma_{2a_t}/\Gamma_{a_t}$ ($\Gamma_{3a_t}/\Gamma_{2a_t}$ for the 1^{-+}) ratios in Table 7, we obtain the mass estimates in the $\delta\mathbf{p}$ column in Table 6. Note that the momentum correction affects the final numbers by $<10\%$. Note also that our final 1^{-+} mass estimate comes from $\Gamma_{3a_t}/\Gamma_{2a_t}$ and hence is particularly reliable.

We conclude that the 1^{-+} oddball is indeed light, being about 10% heavier than the 2^{++}, and that the 0^{--}, which, within its errors, might have been light on the basis of our $\mathbf{p}=0$ estimates alone, is indeed rather heavy, and hence of less interest.

III. Thermal Loops and Metastable States

In setting up our lattice calculations we have been careful to ensure that finite size effects should be under control, in particular we insisted that the spatial extent of the lattice should satisfy

$$L_s a_s \gtrsim 2D_G, \tag{65}$$

where D_G is our estimate of the glueball diameter. We also made sure that the timelike extent of the lattice, $L_t a_t$, should be such that the temperature, T, of the lattice is always well below the deconfining temperature, T_c:

$$T\left(=\frac{1}{L_t a_t}\right) \ll T_c \approx 200\,\text{MeV}. \tag{66}$$

The absence of severe finite-size effects is implied by the approximate continuum renormalization group behaviour we found for the 0^{++} and 2^{++} masses in a region of couplings, where the lattice spacing, and hence the spatial lattice extent also, more than doubles in size. Further evidence comes from the $SU(2)$ case where we obtained [5] consistent mass estimates on $4^3 \cdot 8$, 8^4 and $5^3 \cdot 40$ lattices in a range of couplings analogous to that being considered in this paper. (The operator projections, α, for the 2×2 loop did show significant changes, as might be expected.)

This is in contrast to (quenched quark) hadron spectrum calculations, where finite size effects on lattices comparable in size to ours have been found [25, 26] to be very large. A prominent part of this effect has found a transparent description in thermodynamic terms [26]: the small spatial extent of the lattice implies a *spatial* temperature around the deconfining transition [27] temperature ($T_c \approx \Lambda_{\text{mom}} = 200\,\text{MeV}$), so that the global $Z(3)$ gauge invariance in spatial directions will be spontaneously broken. This is to say that spatial thermal loops (spatial loops that close through the periodic boundaries) will pick up a corresponding $Z(3)$ phase factor, and a quark propagating through a boundary will pick up a corresponding phase relative to one that does not, and hence the meson propagator, consisting of a product of quark and antiquark propagators, will pick up pieces with interfering phases when one of the quarks loops through the boundary (or when both do so through differing boundaries). All this then raises the question of whether similar thermodynamic effects might not be affecting our glueball mass calculations.

The first point to make is that for a meson or baryon calculation our criterion (65) is *grossly* violated for a lattice that is comparable in size to the $4^3 \cdot 8$ lattice at $\beta = 5.7$. Indeed, since $D_H \simeq 1-2$ fermi (the subscript H standing for hadron), it is reversed (!):

$$\tfrac{1}{2} L_s a_s = 2a(\beta = 5.7) < D_H. \tag{67}$$

Hence the presence of strong finite size effects was to be expected.

The second point is that the effect on meson and baryon propagators as described in the previous paragraph is actually a straightforward consequence of (67). When both q and $\bar{q}$ propagators go through the same boundary, the $Z(3)$ phase factor cancels in the product. Hence the effect only arises when the q, $\bar{q}$ propagate through differing boundaries (or when only one goes through a boundary), and this requires the q, $\bar{q}$ inside the propagating meson to be a distance $\simeq L_s a_s$ apart at some point, which *cannot*

happen if (65) is valid (confinement) and only happens because (65) is badly violated, as in (67). So if the hadron calculations had been performed under the constraint (65), as our glueball calculations have been, they would not show the above effects.

The third point is that a propagating gluon, being a colour octet, will not pick up any $Z(3)$ phase factor even when it passes through a spatial boundary. Hence the particular problem we have described would not afflict our glueball calculations, even if we had been so careless as to neglect imposing (65) upon our choice of lattice.

The above problem of "fake" loops [25, 26], which we have shown to be irrelevant to our glueball calculations, is, however, a relatively superficial, even if readily visible, one. The same thermodynamic language points to a more pertinent question: the spontaneous breaking of the global $Z(3)$ symmetry implies that the characteristic configurations of the vacuum are now *systematically* different to

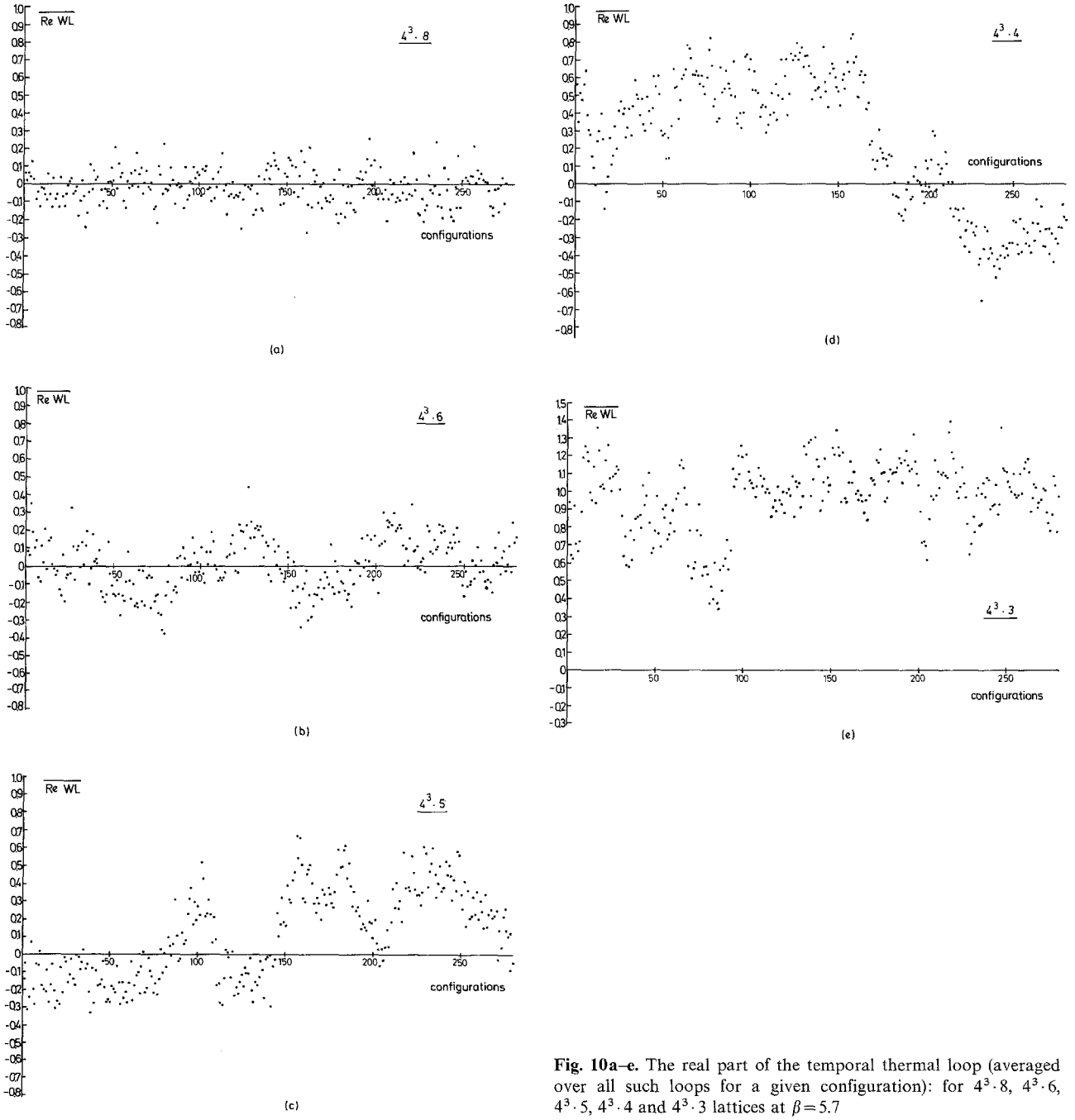

Fig. 10a–e. The real part of the temporal thermal loop (averaged over all such loops for a given configuration): for $4^3 \cdot 8$, $4^3 \cdot 6$, $4^3 \cdot 5$, $4^3 \cdot 4$ and $4^3 \cdot 3$ lattices at $\beta = 5.7$

those in the symmetric phase – how does this affect meson/baryon/glueball masses? Of course, these masses will be independent of which "$Z(3)$" vacuum we are in (neglecting explicit finite-size effects, where quarks loop through boundaries). However, they certainly need not be the same as in the symmetric phase. This is a question relevant to all mass calculations – and needs to be addressed in quark calculations just as seriously as the question of fake loops.

To help to clarify the above question, we have calculated expectation values of the thermal loops, in all four directions, on $4^3 \cdot 8$, $4^3 \cdot 6$, $4^3 \cdot 5$, $4^3 \cdot 4$, $4^3 \cdot 3$, $4^3 \cdot 2$ lattices at $\beta = 5.7$. We choose this value of β since it is the most relevant one for the bulk of our mass estimates. In Fig. 10a–e we plot the real part of the thermal loop in the time direction for these lattices. For each configuration we average the real parts of the 4^3 parallel temporal thermal loops, and we plot this value for a sequence of ≈ 300 gauge field configurations for each lattice size. The spontaneous breaking of the temporal $Z(3)$ symmetry will be apparent in that the $\overline{\mathrm{Re}\, WL}$ should remain fixed in one of three values corresponding to a phase for the loop of 0 or $\pm 2\pi/3$. The onset of the phase transition will be apparent in that $\overline{\mathrm{Re}\, WL}$ will oscillate between these values with an increasing wavelength (in terms of the number of configurations) as the system passes through the transition to the broken symmetry phase. From Fig. 10 we conclude:

(i) on a $4^3 \cdot 8$ lattice the temporal $Z(3)$ symmetry is *not* spontaneously broken;

(ii) the phase transition occurs in a smooth fashion as we change L_t from $L_t = 6$ to $L_t = 3$; this corresponds to a width of $\Delta T \simeq 150\,\mathrm{MeV}$ for a phase transition which in the large (spatial) volume limit attains a zero width.

The first observation tells us that the physical system described by the transfer matrix, which takes us between equal time slices, on the $4^3 \cdot 8$ lattice is in the desired confining phase. That is to say, our glueball mass estimates were indeed made for the low temperature gauge theory. The second observation suggests that for a lattice as small as the present one the thermodynamic language (with its precise phases and phase transitions) has become too obscure to be very useful. Probably our more direct finite-size approach, as embodied in (65), is more appropriate.

For completeness, in Fig. 11 we plot for the $4^3 \cdot 8$, $4^3 \cdot 6$ and $4^3 \cdot 3$ lattices the average over the real parts of the $4^3 \cdot (8, 6, 3)$ thermal loops pointing in the x direction and, separately, for those pointing in the y direction. We conclude:

(i) the level of metastability in the spatial $Z(3)$ symmetry is appropriate to the onset of a broad phase transition to a spontaneously broken phase;

(ii) the degree of spatial $Z(3)$ metastability is independent of the temporal length of the lattice;

(iii) the degree of metastability in the x direction is independent of that in the y direction.

We describe now a direct search for evidence of metastable states, which possess differing glueball properties. We perform the search on our 6,000 $4^3 \cdot 16$ gauge field configurations. Our procedure is to split the data up into batches of 100 sequential configurations, to calculate $\Gamma_{na_t}/\Gamma_{(n-1)a_t}$ for each such batch and finally to plot the results and to search for a multiple peak structure in the plotted distribution. A statistically significant multiple peak structure would indicate the presence of metastable states of a lifetime $\tau \gtrsim 100$ configurations. We repeat the

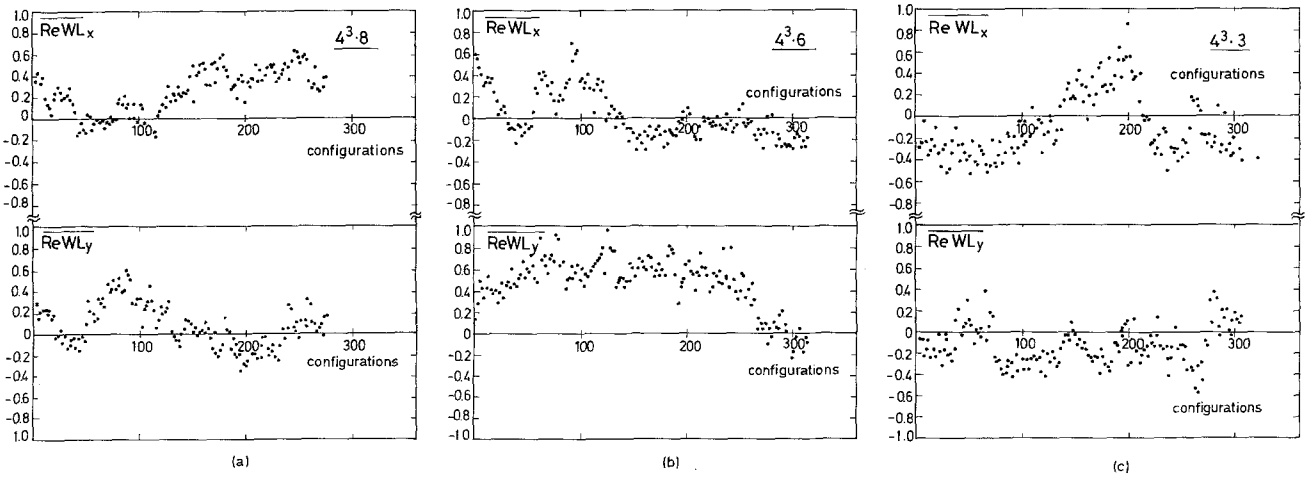

Fig. 11a–c. As in Fig. 10, but for thermal loops in the spatial (x and y) ditections and for $4^3 \cdot 8$, $4^3 \cdot 6$ and

exercise for batches of 200 and 400 sequential configurations. The resulting distributions will be sensitive to metastable states with lifetimes $\tau \simeq 200$ and 400 configurations, respectively. The reason for doing so is that the statistical fluctuations on Γ_{a_t}/Γ_0 will decrese as the batch length increasses, enabling us to discern peaks that may be closer together (although increasing the batch length reduces the number of batches, and this will tend to counteract this improvement).

In Fig. 12 we plot the distribution of the 0^{++} $\Gamma_{3a_t}/\Gamma_{2a_t}$ ratio for batches of 200 and 400 iterations. We have thirty such batches obtained by using both the 6 and 12 link operators. Since $\Gamma_{3a_t}/\Gamma_{2a_t} = e^{-ma_t}$, any significant structure in these distributions would be a reflection of metastable states with differing 0^{++} masses. We see no such statistically significant effect for batches of length 400. The only possible candidate, the peak around 0.65–0.70, should be more pronounced, if real, for batches of 200. But it is not there. For batches of 200 the statistical fluctuations are large. In fact there is an entry at -0.63 (!), which we have omitted for presentation reasons. It is probably reasonable to conclude that any important metastable states of lifetime $\gtrsim 400$ iterations have average $\Gamma_{3a_t}/\Gamma_{2a_t}$ values between 0.4 and 0.55, i.e. the masses of different such metastable states are confined to a region

$$ma_t \simeq 0.60 - 0.92. \tag{68}$$

In Fig. 13 we plot Γ_{a_t}/Γ_0 for the 6 link 2^{++} operator for batches of 100, 200 and 400 configurations. Γ_{a_t}/Γ_0 reflects a mixture of mass and wavefunction factors. We would prefer to use $\Gamma_{2a_t}/\Gamma_{a_t}$, but the statistical fluctuations would certainly mask any structure. We observe an obvious secondary candidate peaking around $\Gamma_{a_t}/\Gamma_0 \approx 0.075$, which is relatively independent of the batch length. Looking at the data in detail, we find that out of the 14 blocks with $\Gamma_{a_t}/\Gamma_0 \leqq 0.09$, 6 belong to a single sequence of 600 configurations, and this sequence possesses a subsequence of 4 blocks with $\Gamma_{a_t}/\Gamma_0 \leqq 0.085$. A probability calculation suggests that this sequence has occurred about 10 to 20 times more frequently than it should have, if it was at random from a single overall Gaussian distribution. The hypothesis suggests itself that the system possesses a main (possibly conglomerate) metastable state with a correlation length of 0 (4,000), and a secondary metastable state, responsible for this secondary peaking, with a correlation length of 500 ± 200 configurations. To test this hypothesis, we have looked at our 0^{++} and 1^{-+} data for these same $\simeq 600$ configurations. There is no signal of any special behaviour. We return to our 2^{++} data and look at the 12 link Γ_{a_t}/Γ_0. We find no comparable

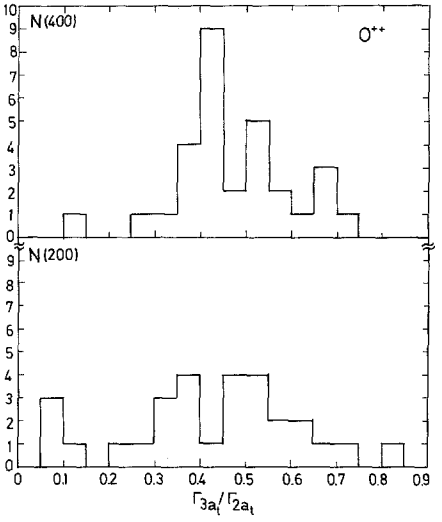

Fig. 12. Distributions of measurements of $\Gamma_{3a_t}/\Gamma_{2a_t}$ on the $4^3 \cdot 16$ lattice for the 0^{++} glueball; the data has been split into sequences of 400 and 200 configurations, respectively

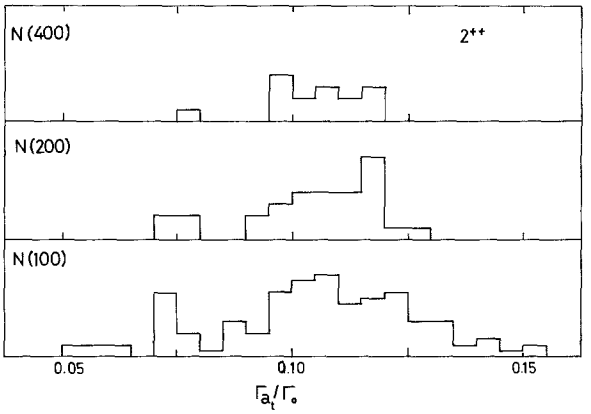

Fig. 13. As in Fig. 12, but for the 2^{++} and Γ_{a_t}/Γ_0, and also with sequences of 100 configurations

behaviour. We conclude that there is no evidence of any metastable state.

A similar conclusion follows from our data on the $4^3 \cdot 8$ lattice. There our data comes from 10 independently initiated and generated sequences of 2,500 to 3,000 configurations. The error on our estimate

$$\Gamma_{2a}/\Gamma_a|_{0^{++}} = 0.361 \pm 0.018 \tag{69}$$

shows directly that any metastable states with lifetimes $\gtrsim 2{,}500$ configurations must possess very similar 0^{++} masses.

The above evidence points to the conclusion that our mass estimates are not being corrupted by high temperature effects. Of course, the ultimate test of this would be to redo the mass calculations on larg-

er lattices. We remind the reader that we have done this indirectly by using the $4^3 \cdot 8$ lattice at smaller β, and directly in the $SU(2)$ case with calculations on $5^3 \cdot 40$ and 8^4 lattices [5].

IV. Discussion and Conclusions

In this final part of the paper we shall begin by comparing our glueball mass estimates with those of [8, 9] and shall resolve the discrepancies.

We shall then return to our rather surprising glueball size estimate, $D_G \approx 0.5$ fermi, and present the arguments for its validity. This is important because our choice of lattice was critically dependent on this estimate.

Finally we shall summarise our most interesting results and mass estimates.

Comparison with Other Calculations

In addition to our work [7], there have also been mass estimates for the bulk of the glueball spectrum by Berg and Billoire [8] and a 0^{++} mass estimate by Michael and Teasdale [9].

The calculation of [8] is on a $4^3 \cdot 8$ hypercubic lattice and uses a variational technique [28] in a way similar to ours. Reference [9] is on a $4^3 \cdot 10$ hypercubic lattice and uses the attenuation with time of an oscillating zero-momentum source (based on the plaquette).

The most interesting states are those of light mass, the 0^{++}, 0^{-+}, 2^{++} and 1^{-+}. For the 0^{++} there is broad agreement (see Fig. 14). For the 0^{-+} ours is the only calculation. For the 2^{++}, however, the authors of [8] claim a severe breaking of continuum renormalization group behaviour, especially in the region $\beta > 5.4$, where, in contrast, we do find scaling (see Fig. 15). The discrepancy between our results and those of [8] is greatest for the 1^{-+} oddball, where their number is 2.5 times greater than our value (see Fig. 16). (The error on the 1^{-+} mass value from [8] is large, and one might be misled into seeing the disagreement as being only $a \approx 2\sigma$ effect. In fact, it is Γ_a/Γ_0, not $ma = \ln \Gamma_0/\Gamma_a$, that has a normal distribution, and if one goes through the logarithm, one can see that the discrepancy is really at the $\approx 7\sigma$ level). Clearly we need to resolve these discrepancies if we are to have confidence in our results.

We begin with the 0^{++} glueball. In Fig. 14 we plot the various mass estimates versus β. As usual we have taken the measured values of $ma(\beta)$ and expressed $a(\beta)$ in terms of a fixed unit, $a(\beta = 5.7)$, using the 2-loop formula, (10). In the resulting plot of $ma(\beta = 5.7)$ continuum behaviour manifests itself

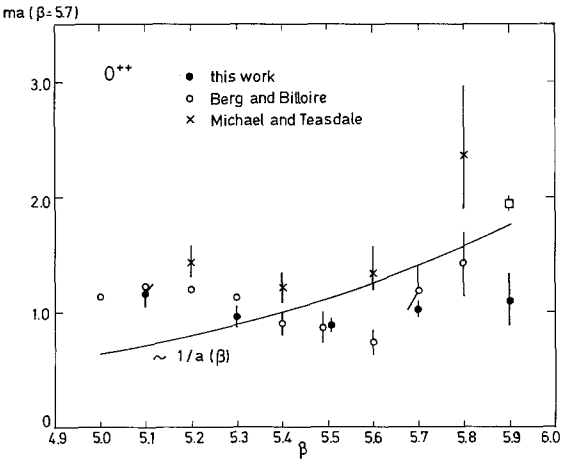

Fig. 14. A compilation of available data on the 0^{++} glueball mass

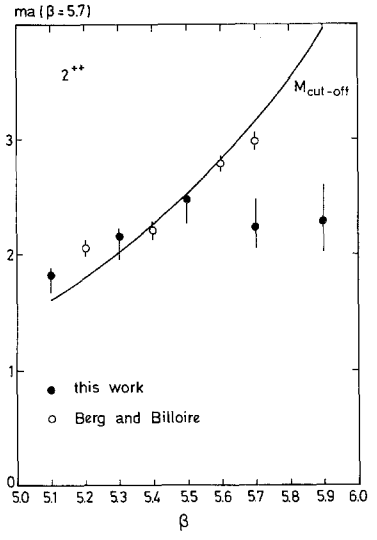

Fig. 15. A compilation of available data on the 2^{++} glueball mass

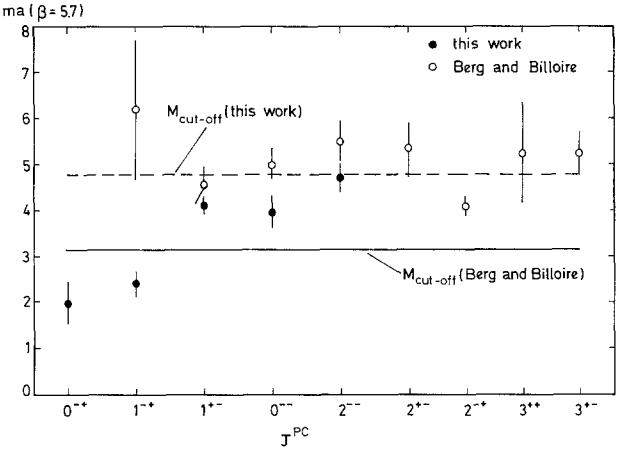

Fig. 16. A comparison of excited glueball mass estimates

as independence of β. We find this preferable to the common alternative of plotting $ma(\beta)$ directly on a semi-log plot, which easily conceals large disagreements. To give a measure of the significance of any apparent constancy, we also plot the β dependence of a mass which is independent of β in *lattice* units, i.e.

$$m \sim \frac{1}{a(\beta)}. \tag{70}$$

Such a behaviour is a typical example of what one might find if one were *not* in the continuum limit. (The data we take from [8] is as follows: for $\beta \geqq 5.4$ the (maximal) Γ_{2a}/Γ_a is used, and for $\beta < 5.4$ the (maximal) Γ_a/Γ_0. From [9] we use: the analogue of Γ_{2a}/Γ_a for $\beta \geqq 5.6$, and $\Gamma_{1.5a}/\Gamma_{0.5a}$ - the half-integer values come from using timelike plaquettes - for $\beta < 5.6$.) We observe an overall consistency between the various mass estimates. There is a trend for the mass estimates of [9] to be somewhat higher than ours or those of [8]. There is also a trend for the mass estimates of [8] and [9] to increase (in GeV units) with β for $\beta > 5.6$. Such a trend is not unexpected: the mass estimates come from Γ_{2a}/Γ_a, and we have found that at $\beta = 5.9$ this has become a poor measure of the mass. We display in Fig. 14 the actual mass estimate (square point) we would obtain from the (maximal) Γ_{2a}/Γ_a ratio at $\beta = 5.9$. It follows well the upward trend of the estimates from [8]. Our 0^{++} mass estimate at $\beta = 5.9$ comes from using Γ_{3a}/Γ_{2a}.

We turn now to our areas of disagreement. In Fig. 15 we plot our estimates of the 2^{++} mass alongside those of [8], again as the dimensionless ratio $ma(\beta = 5.7)$. We also plot the quantity

$$M_{\text{cut-off}} = \frac{\pi}{a(\beta)} \cdot a(\beta = 5.7), \tag{71}$$

which is a measure of the highest mass for which the coarse $4^3 \cdot 8$ lattice can be considered reliable. We note that the mass estimates of [8] are close to $M_{\text{cut-off}}$ and show a strong β dependence for $\beta > 5.4$, in contrast to our mass estimates. We also note that where our mass estimates appear to show some β dependence, for $\beta \leqq 5.3$, $M_{\text{cut-off}}$ has sunk below the higher β 2^{++} mass estimates. This corroborates our earlier suggestion that for $\beta \leqq 5.3$ the 2^{++} glueball changes into a lattice rather than continuum object.

In Fig. 16 we plot the glueball mass estimates of [8], other than the 0^{++} and 2^{++}. We also plot $M_{\text{cut-off}}$ for this data (solid line). (The data [8] comes from $\beta = 5.7$ where possible; for the 0^{--} and 3^{+-} this was not possible, so we used mass-estimates taken [8] at $\beta = 5.6$.) In the same figure we plot our excited glueball mass estimates, as obtained on the $4^3 \cdot 16$ space-time asymmetric lattice. We plot $M_{\text{cut-off}}$ for this data (dashed line). Since the temporal lattice spacing is smaller, the $4^3 \cdot 16$ lattice should in principle be more reliable for higher masses. We observe that all our mass estimates lie *below* the corresponding ones from [8], the 1^{-+} being the most dramatic example. We also note that our mass estimates have a much healthier relation to their $M_{\text{cut-off}}$ than do those of [8].

The resolution of all these disagreements lies in a simple observation: *all* the excited glueball mass estimates of [8] are obtained from Γ_a/Γ_0. This is in contrast to our estimates, which (for $\beta \gtrsim 5.5$) all use Γ_{2a}/Γ_a or even Γ_{3a}/Γ_{2a}. (Where we have used Γ_a/Γ_0 for $\beta \leqq 5.5$, we have always been careful to estimate wavefunction corrections and to include these with generous errors, as in Fig. 5.) Suppose we write

$$\frac{\Gamma_a}{\Gamma_0} = \alpha(\beta) e^{-ma(\beta)}, \tag{72}$$

then the mass estimate, m, one obtains from this ratio, is

$$\tilde{m} = m + \frac{1}{a(\beta)} \ln \left[\frac{1}{\alpha(\beta)} \right]. \tag{73}$$

As β increases not only does $a(\beta)$ decrease, but so does $\alpha(\beta)$, and rapidly. This is true even if one performs a variational improvement of a *fixed* (with β) subset of trial wave-functionals (see Fig. 5). Hence m will increasingly overestimate m as β increases. (In reality the situation is worse; at larger β we must include higher mass contributions in (72).) It is clear that the discrepancy will become worse sooner the lighter is m.

The disagreement between our masss estimates and those of [8] follow this pattern exactly: for increasing β the disagreement grows rapidly, and for higher mass states it is relatively smaller. As a final check we take *our* measured values of Γ_a/Γ_0, and find that if we use these to obtain mass estimates, then indeed the discrepancies disappear.

It is clear then that the higher β mass estimates of [8] for excited glueballs should really be seen as mass *upper-bounds*, and as such they are no longer in disagreement with our estimates.

On the Size of the 0^{++} Glueball

We have estimated the mean glueball diameter to be:

$$D_G \approx (1.5 - 2.0)\, a(\beta = 5.7)$$
$$\approx 0.5 \text{ fermi}. \tag{74}$$

This is in contrast to normal meson and baryon sizes,

$$D_{M/B} \simeq 1-2 \text{ fermi} \simeq (4-8)\, a(\beta=5.7), \tag{75}$$

and raises the question of how confident we can be of our estimate for D_G.

The most naive possibility is that we might have our GeV scale wrong. If in fact $\Lambda_{\text{mom}} \simeq 70$ MeV rather than 200 MeV, the D_G becomes $\simeq 1.5$ fermi. However such a Λ_{mom} would give wildly wrong predictions for the gluon condensate and string tension, and it would wreck quenched QCD hadron spectrum calculations which generally prefer a larger Λ_{mom} than 200 MeV. Accordingly we discard this possibility.

The only other way that D_G could be equal to $D_{M/B}$ is if we were wrong in our estimate of D_G in terms of lattice units, i.e. $D_G \simeq (4\text{-}8)\ a(\beta=5.7)$ rather than (74). We take this possibility seriously and give arguments why we believe it to be incorrect.

Our original evidence for (74) came from Fig. 2: the better an operator mimics the glueball wavefunction, the bigger will be its projection and hence the bigger should be Γ_a/Γ_0. Hence the position of the maximum in Γ_a/Γ_0 plotted versus the size of the operator should give a reasonable estimate of the glueball size. We note that the glueball size estimates obtained in this way vary by no more than $\approx 15\%$ over a range of β values corresponding to the lattice spacing, and total lattice size, varying by $\approx 100\%$. This is impressive evidence for the correctness of our procedure and simultaneously for the renormalization group behaviour of the 0^{++} glueball size. Secondly we observe that if D_G was really $\simeq 4a(\beta=5.7)$, then, as we decrease β so that the glueball fits more easily into the enlarging lattice, the similarly growing (in GeV^{-1} units) 2×2 loop should rapidly become a good trial wave-functional. What we observe instead is completely the opposite behaviour.

If we still wish to continue our pursuit of a larger glueball, we must at this point discard the evidence of Fig. 2. That is to say, we must claim that the operators are all very bad approximations to the true 0^{++} wavefunction, so that they are dominated by higher mass states, and what we see is some obscure reflection of that. This however completely contradicts our estimates for the goodness of our operators as obtained by comparing Γ_a/Γ_0 with Γ_{2a}/Γ_a; see Fig. 5.

To continue along this line we must therefore assume that in fact Γ_{2a}/Γ_a is also dominated by higher mass states and not by the lowest 0^{++} glueball mass as we assumed. That is to say, if we plot the effective mass obtained as

$$m_{\text{eff}}(n)\, a_t = \ln \frac{\Gamma_{(n-1)a_t}}{\Gamma_{na_t}}, \tag{76}$$

then at $n=2$ this should still be a rapidly decreasing function of n. Our direct measurements on the $4^3 \cdot 16$ lattice, as shown in Fig. 9, show no such decrease. Rather they support the assumption that $\Gamma_{2a_t}/\Gamma_{a_t}$ is dominated by the lowest glueball mass. (Recall that the temporal lattice spacing on the $4^3 \cdot 16$ lattice is $3a_t \approx 2a(\beta=5.7)$.)

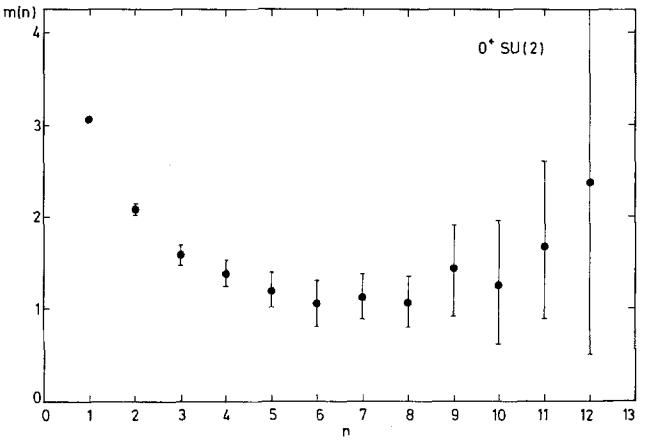

Fig. 17. As in Fig. 9 for the 0^+ in $SU(2)$ on a $5^3 \cdot 40$ lattice

As final evidence we present in Fig. 17 the result of calculating $m_{\text{eff}}(n)$ on a $5^3 \cdot 40$ lattice with $a_t = 1/4a_s$ for the $SU(2)$ 0^+ glueball [5]. This calculation demonstrated very clearly that in the $SU(2)$ case, for a region of couplings precisely analogous to that being considered here,

$$\frac{\Gamma_{2a}}{\Gamma_a} \approx \frac{\Gamma_{8a_t}}{\Gamma_{4a_t}} \tag{77}$$

does indeed accurately reflect the lowest 0^+ glueball mass.

All of this leads us back to our original estimate of D_G in (74).

Conclusions

We have calculated the masses of the lowest-lying 0^{++}, 2^{++}, 0^{-+}, 1^{+-}, 1^{-+}, 0^{--}, 2^{--} glueballs in the $SU(3)$ lattice-regularized non-abelian gauge theory. (Of course, our operators cannot be *pure* J^{PC} wavefunctionals: for example, both the 0^{++} and 2^{++} operators possess admictures of 4^{++}. If however the 4^{++} glueball were lighter than the 0^{++}, we should

have obtained equal "0^{++}" and "2^{++}" masses, which we did not.)

We have shown that both the 0^{++} and 2^{++} adhere to a statistically significant extent to the desired continuum renormalization group behaviour, implying that they are indeed representative of the continuum gauge theory. This reflects favourable upon the validity of our other states, for which we have not yet performed such a calculation.

Using the string tension as our scale ($\Lambda_{\text{mom}} = 200\,\text{MeV}$), we summarise our mass estimates in MeV units:

$$\begin{aligned} m(0^{++}) &= 740 \pm 40\,\text{MeV} \\ m(0^{-+}) &= 1420\,{}^{+240}_{-170}\,\text{MeV} \\ m(2^{++}) &= 1620 \pm 100\,\text{MeV} \\ m(1^{-+}) &= 1730 \pm 220\,\text{MeV} \\ m(0^{--}) &= 2880 \pm 300\,\text{MeV} \quad \text{oddballs} \\ m(2^{--}) &= 3420 \pm 300\,\text{MeV} \\ m(1^{+-}) &= 2980 \pm 300\,\text{MeV} \end{aligned} \tag{78}$$

We have thus found four light glueballs, the scalar 0^{++}, pseudoscalar 0^{-+}, tensor 2^{++} and the oddball 1^{-+}. These should be of special phenomenological interest, especially the light oddball. The fact that we find that the typical glueball diameter is only about 0.5 fermi should also have interesting implications for glueball production and mixing.

Acknowledgements. We thank various colleagues at DESY and Hamburg for useful discussions and comments. We also thank P. Hasenfratz and M. Lüscher for their critical questions. The computer calculations were performed at DESY and at LICEPP, University of Tokyo. We are grateful to both institutions for the allocation of computer time. One of us (M.T.) is grateful to T. Walsh for the hospitality of the DESY theory group several times during the course of this work. Another of us (K.I.) has been supported in part by NSF grant PHYS-78-2488 and in part by a CUNY FRAP Award.

Note Added. After completion of this paper we received a preprint by Berg and Billoire (Saclay preprint SPh.T/42), which repeats their previous $SU(3)$ calculation (8) on a slightly larger $5^3 \cdot 8$ lattice. Moreover they systematically consider all operators of length up to 8 links. They find finite size effects for Γ_0, but not for the mass estimates (a possible effect is an increase of the 0^{++} mass at $\beta = 5.6$, but it is a $\lesssim 2\sigma$ effect and so not very significant). We recall our own finite size studies [5, 6] in $SU(2)$, in an analogous range of couplings, on $4^3 \cdot 8$, $5^3 \cdot 40$, 6^4 and 8^4 lattices. While we found some changes in Γ_a/Γ_0, we did not observe any changes in the mass estimates. For the excited states they find no continuum behaviour, and the mass estimates are systematically (much) higher than ours (as in the $4^3 \cdot 8$ case), including now a 0^{-+} estimate. This is to be expected since all these mass estimates are obtained using Γ_a/Γ_0 rather than Γ_{2a}/Γ_a, just as in their $4^3 \cdot 8$ calculation [8], and it re-emphasises the necessity of taking measurements further out along the correlation function as one probes deeper into the continuum limit: a pure variational calculation is not enough!

Appendix

A Comparison of Different Random Number Generators

The Monte Carlo procedure generates a sequence of gauge field configurations from an underlying sequence of random numbers. The randomness of these numbers is necessary to ensure that any configuration is eventually accessible, and that these configurations should indeed be generated with the correct weighting as given by the exponential of the action.

In practice the computer generates the sequence of "random numbers" from some well-defined algorithm, and hence they are not truly random. It is conventional to call them pseudorandom [23]. These pseudorandom numbers possess (weak) correlations, which will perturb our Markovian Monte Carlo procedure. The general problem is analogous to the stability problem of a highly non-linear system under a weak perturbation. Two pertinent questions are: (i) are "asymptotic" values of correlation functions affected by these perturbations? (ii) are statistical errors smaller with some standard generators than with others?

The first question has been addressed previously [4] within the context of some relatively simple exactly soluble models in statistical physics. We shall investigate both questions within the context of our glueball mass calculations, following a brief discussion of pseudorandom numbers.

Pseudorandom Numbers [23]

Sequences of pseudorandom numbers are not infinite but periodic with a period that is typically $O(2^t)$, where t is the number of bits used for integer representation. For a 32 bit machine (e.g. IBM) this is $O(10^9)$, while for a 60 bit machine (e.g. CDC) this is $O(10^{17})$. A typical long calculation of the type desired in this paper uses $O(10^9)$ random numbers. This suggests taking the precaution of working with a double-precision generator on a 32 bit machine. A period of $O(10^{17})$ may be considered infinite in the context of any conceivable lattice calculation.

An interesting manifestation of the correlations in a sequence of pseudorandom numbers is the Marsaglia effect [29]: group successive members of the sequence into n-triples and regard these n-triples as specifying the coordinates of a point in n dimen-

sional space. One finds that these points are not distributed randomly in this space. Instead they lie in a finite (n-dependent) number of hyperplanes. For $n=2$ or 3 this effect is, by design, very weak. But for $n=O(20)$ it typically becomes significant. One might imagine that, within our context, this could manifest itself in the non-uniform population of colour space and correlations between the colour orientations of different links. Since different generators manifest these effects to a greater or lesser extent, one can search for the impact of these correlations by comparing calculations with different generators. This we now do.

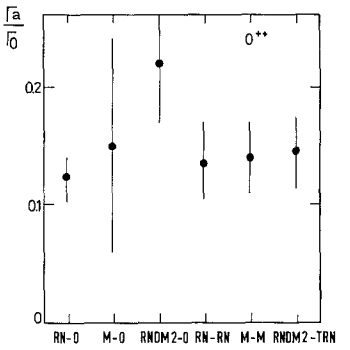

Fig. 18. Γ_a/Γ_0 for the 0^{++} with various random number generators and upgrading procedures

Numerical Comparison

We work on a $4^3 \cdot 8$ lattice at $\beta=5.7$. We calculate Γ_a/Γ_0 (defined in (7)) for 0^{++}, 2^{++} and 1^{+-} glueballs, using $\mathbf{p}=0$ wavefunctions constructed out of the simple plaquette. We perform six independent such calculations using different generators and updating procedures, labelled by $X-Y$. $X \in \{\mathrm{RN}, \mathrm{M}, \mathrm{RNDM2}\}$ specifies (see below) which of three pseudorandom number generators was used for updating the link matrices and Y specifies how the link to be updated is chosen. If $Y=0$, then the choice is sequential (ordered), otherwise the choice is at random and Y specifies the (pseudo)random numbers used.

The combinations of $X-Y$ tested are RN-0, M-0, RNDM2-0, RN-RN, M-M and RNDM2-TRN. Here RN is a standard 32 bit multiplicative congruential generator [23], RNDM2 is a 60 bit such generator [30], and M is a generator [31] designed to exhibit no Marsaglia effect up to $n=16$. TRN is a sequence of 10^7 *true*, physically generated, random numbers [22]. This sequence is too short for link updates but is long enough to use for the random choice of which link to update next.

For each combination of $X-Y$ we generate 300 configurations to reach equilibrium and then a further 800 configurations for measuring Γ_a/Γ_0.

The various values of Γ_a/Γ_0 for 0^{++} and 2^{++} show no significant differences within the statistical errors. In Fig. 18 we show, for example, the measurements for 0^{++}.

The values of Γ_a/Γ_0 for the 1^{+-} state are plotted in Fig. 19 as solid circles. There is a large, though not significant, scatter of points. What appears more significant is the variation of the sizes of the statistical errors on these points. To clarify this question, we have taken what look like two extreme cases, RN-0 and RNDM2-TRN, and we have performed measurements on a further set of 3,000 configurations in each case. The results are the solid triangles in Fig. 19. We observe that in each case the

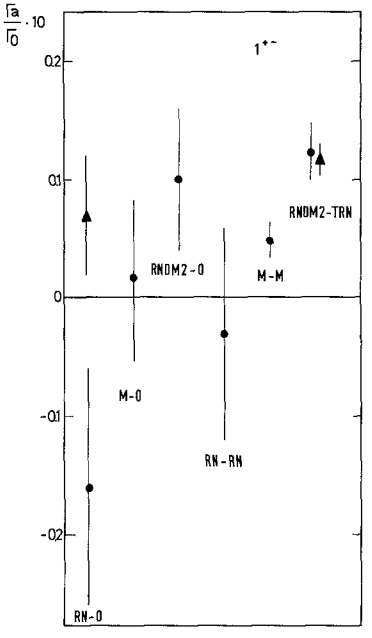

Fig. 19. A study of the dependence of Γ_a/Γ_0 for the 1^{+-} for various random number generators and upgrading procedures

errors have been reduced by about a factor of 2 for an increase in the number of measurements by about a factor of 4. This is as expected and indicates that our error estimates are accurate. (Studies of our other data indicate that the errors on these error estimates are not more than $O(30\%)$.) All this leaves us with rather strong evidence that statistical errors can depend strongly on the generator/updating procedure employed. In the present example of the 1^{+-} state the error using RNDM2-TRN is a factor 4 to 5 smaller than the error with RN-0. In other words, using the latter procedure, we need ≈ 20 times more events for the same statistical accuracy!

We now address the crucial question of whether the actual "asymptotic" values vary with the $X-Y$

procedure employed. We have seen already (in the main body of the paper) that the mass ratios of the 0^{++}, 2^{++} and 0^{-+} glueballs are the same (within errors) in the two independent calculations on $4^3 \cdot 8$ and $4^3 \cdot 16$ lattices. Since the former used RN-0, while the latter used RNDM2-TRN, this indicates that at least these states are stable under the perturbations induced by the use of pseudorandom, rather than truly random, numbers. The situation with the 1^{+-} state is more delicate. Comparing Γ_a/Γ_0 for 1^{+-} using RN-0 on about 27,000 configurations with the RNDM2-TRN value (3,000 configurations) suggests a discrepancy at the $\approx 3\sigma$ level. This is worrisome but not conclusive.

References

1. H. Fritzsch, M. Gell-Mann, H. Leutwyler: Phys. Lett. **47B**, 365 (1973)
2. K. Wilson: Phys. Rev. **D10**, 2445 (1974)
3. M. Creutz: Phys. Rev. Lett. **43**, 553 (1979); K. Wilson: Cargèse Lectures 1979; M. Creutz, L. Jacobs, C. Rebbi: Phys. Rev. **D20**, 1915 (1979)
4. K. Binder: In: Phase transitions and critical phenomena. Vol. 56. eds. C. Domb, M.S. Green. New York, London: Academic Press 1976; K. Binder (Ed.): Monte Carlo methods in statistical physics. Berlin, Heidelberg, New York: Springer 1979
5. K. Ishikawa, G. Schierholz, M. Teper: Z. Phys. C - Particles and Fields **19**, 327 (1983)
6. K. Ishikawa, G. Schierholz, M. Teper: Phys. Lett. **110B**, 399 (1982); Z. Phys. C - Particles and Fields **16**, 69 (1982)
7. K. Ishikawa, G. Schierholz, M. Teper: Phys. Lett. **116B**, 429 (1982); K. Ishikawa, A. Sato, G. Schierholz, M. Teper: Phys. Lett. **120B**, 387 (1983)
8. B. Berg, A. Billoire: Phys. Lett. **113B**, 65 (1982); Phys. Lett. **114B**, 324 (1982); DESY preprint DESY 82-079
9. C. Michael, I. Teasdale: Nucl. Phys. **B215**, 433 (1983)
10. M. Lüscher: Commun. Math. Phys. **54**, 283 (1977); K. Osterwalder, E. Seiler: Ann. Phys. **110**, 440 (1978)
11. A. Hasenfratz, P. Hasenfratz: Nucl. Phys. **B193**, 210 (1981); and references therein
12. M. Creutz: Phys. Rev. Lett. **45**, 313 (1980); E. Pietarinen: Nucl. Phys. **B190**, 349 (1981); M. Creutz, K. Moriarty: Phys. Rev. **D26**, 2166 (1982); E.-M. Ilgenfritz, M. Müller-Preussker: Dubna preprint E2-82-473 (1982)
13. M.A. Shifman, A.I. Vainshtein, V.I.I. Zakharov: Nucl. Phys. **B147**, 385, 519 (1979)
14. E.M. Ilgenfritz, M. Müller-Preussker: Phys. Lett. **119B**, 395 (1982)
15. S.N. Nikolaev, A.V. Radyushkin: Nucl. Phys. **B213**, 285 (1983)
16. This straightforward but crude procedure proves, in the $SU(2)$ case, to be in accord with the results of a more detailed investigation of glueball structure: K. Ishikawa, G. Schierholz, H. Schneider, M. Teper: DESY preprint DESY 82-087/LAPP-TH 70 (1982); Nucl. Phys. **B**
17. F. Karsch: Nucl. Phys. **B205**, 285 (1982)
18. B. Lautrup, M. Nauenberg: Phys. Rev. Lett. **45**, 1755 (1980)
19. M. Creutz: Phys. Rev. Lett. **46**, 1441 (1981); K. Moriarty: Phys. Lett. **106B**, 130 (1981); H. Bohr, K. Moriarty: Phys. Lett. **104B**, 217 (1981); M. Creutz and K. Moriarty: Phys. Rev. **D25**, 1724 (1982)
20. G. Münster: Nucl. Phys. **B190**, 439 (1981); **B205**, 648 (1982); Bern preprint BUTP-21/1982 (1982); J. Smit: Nucl. Phys. **B206**, 309 (1982); K. Seo: Nucl. Phys. **B209**, 200 (1982)
21. P. DiVecchia, K. Fabricius, G.C. Rossi, G. Veneziano: Nucl. Phys. **B192**, 392 (1981)
22. Y. Yoshizawa et al.: MIKY tape, Hiroshima University
23. For a discussion of random number generators in the context of conventional (non-Markovian) Monte Carlo calculations see: F. James: Monte Carlo theory and practice. CERN report DD/80/6 (1980)
24. A. Abramowitz, I. Stegun: Handbook of mathematical functions. New York: Dover, 1965
25. P. Hasenfratz, I. Montvay: Phys. Rev. Lett. **50**, 309 (1983)
26. G. Martinelli, G. Parisi, R. Petronzio, F. Rapuano: Phys. Lett. **122B**, 283 (1983); R. Gupta, A. Patel: Phys. Lett. **124B**, 94 (1983)
27. L.D. McLerran, B. Svetitsky: Phys. Lett. **98B**, 195 (1981); Phys. Rev. **D24**, 450 (1981); J. Kuti, J. Polonyi, K. Szlachanyi: Phys. Lett. **98B**, 199 (1981); J. Engels, F. Karsch, I. Montvay, H. Satz: Phys. Lett. **101B**, 89 (1981); **102B**, 332 (1981); Bielefeld preprint BI-TP 81/29 (1981); I. Montvay, E. Pietarinen: DESY preprint DESY 81-077
28. As suggested originally in: K.G. Wilson: Closing remarks at the coseners house lattice meeting. (Abingdon, U.K., March 1981)
29. G. Marsaglia: Proc. Nat. Acad. Sci. **61**, 25 (1968)
30. Written by Marsaglia: see [23]
31. M. Fushimiz, S. Tezuka: Univ. Tokyo Tech. Rept. METR 81-5 (1981)